9 The strong coupling α_{s}

Authors: R. Horsley, T. Onogi, R. Sommer

9.1 Introduction

The strong coupling $\bar{g}_s(\mu)$ defined at scale μ, plays a key role in the understanding of QCD and in its application to collider physics. For example, the parametric uncertainty from α_s is one of the dominant sources of uncertainty in the Standard Model prediction for the $H \to b\bar{b}$ partial width, and the largest source of uncertainty for $H \to gg$. Thus higher precision determinations of α_s are needed to maximize the potential of experimental measurements at the LHC, and for high-precision Higgs studies at future colliders and the study of the stability of the vacuum [1–8]. The value of α_s also yields one of the essential boundary conditions for completions of the standard model at high energies.

In order to determine the running coupling at scale μ

$$\alpha_s(\mu) = \frac{\bar{g}_s^2(\mu)}{4\pi} \, , \tag{279}$$

we should first "measure" a short-distance quantity $\mathcal{Q}$ at scale μ either experimentally or by lattice calculations, and then match it to a perturbative expansion in terms of a running coupling, conventionally taken as $\alpha_{\overline{\mathrm{MS}}}(\mu)$,

$$\mathcal{Q}(\mu) = c_1 \alpha_{\overline{\mathrm{MS}}}(\mu) + c_2 \alpha_{\overline{\mathrm{MS}}}(\mu)^2 + \cdots . \tag{280}$$

The essential difference between continuum determinations of α_s and lattice determinations is the origin of the values of $\mathcal{Q}$ in Eq. (278).

The basis of continuum determinations are experimentally measurable cross sections or decay widths from which $\mathcal{Q}$ is defined. These cross sections have to be sufficiently inclusive and at sufficiently high scales such that perturbation theory can be applied. Often hadronization corrections have to be used to connect the observed hadronic cross sections to the perturbative ones. Experimental data at high μ, where perturbation theory is progressively more precise, usually have increasing experimental errors, and it is not easy to find processes that allow one to follow the μ-dependence of a single $\mathcal{Q}(\mu)$ over a range where $\alpha_s(\mu)$ changes significantly and precision is maintained.

In contrast, in lattice gauge theory, one can design $\mathcal{Q}(\mu)$ as Euclidean short-distance quantities that are not directly related to experimental observables. This allows us to follow the μ-dependence until the perturbative regime is reached and nonperturbative "corrections" are negligible. The only experimental input for lattice computations of α_s is the hadron spectrum which fixes the overall energy scale of the theory and the quark masses. Therefore experimental errors are completely negligible and issues such as hadronization do not occur. We can construct many short-distance quantities that are easy to calculate nonperturbatively in lattice simulations with small statistical uncertainties. We can also simulate at parameter values that do not exist in nature (for example, with unphysical quark masses between bottom and charm) to help control systematic uncertainties. These features mean that precise results for α_s can be achieved with lattice gauge theory computations. Further, as in the continuum, the different methods available to determine α_s in lattice calculations with different associated systematic uncertainties enable valuable cross-checks. Practical limitations are discussed in

the next section, but a simple one is worth mentioning here. Experimental results (and therefore the continuum determinations) of course have all quarks present, while in lattice gauge theories in practice only the lighter ones are included and one is then forced to use the matching at thresholds, as discussed in the following subsection.

It is important to keep in mind that the dominant source of uncertainty in most present day lattice-QCD calculations of α_s are from the truncation of continuum/lattice perturbation theory and from discretization errors. Perturbative truncation errors are of particular concern because they often cannot easily be estimated from studying the data itself. Further, the size of higher-order coefficients in the perturbative series can sometimes turn out to be larger than naive expectations based on power counting from the behaviour of lower-order terms. We note that perturbative truncation errors are also the dominant source of uncertainty in several of the phenomenological determinations of α_s.

The various phenomenological approaches to determining the running coupling, $\alpha_{\overline{\rm MS}}^{(5)}(M_Z)$ are summarized by the Particle Data Group [9]. The PDG review lists five categories of phenomenological results used to obtain the running coupling: using hadronic τ decays, hadronic final states of e^+e^- annihilation, deep inelastic lepton–nucleon scattering, electroweak precision data, and high energy hadron collider data. Excluding lattice results, the PDG quotes the weighted average as

$$\alpha_{\overline{\rm MS}}^{(5)}(M_Z) = 0.1174(16), \quad \text{PDG 2018 [9]} \tag{281}$$

compared to $\alpha_{\overline{\rm MS}}^{(5)}(M_Z) = 0.1183(12)$ of the older review [10]. For a general overview of the various phenomenological and lattice approaches see, e.g., Ref. [11]. The extraction of α_s from τ data, which is the most precise and has the largest impact on the nonlattice average in Eq. (279) is especially sensitive to the treatment of higher-order perturbative terms as well as the treatment of nonperturbative effects. This is important to keep in mind when comparing our chosen range for $\alpha_{\overline{\rm MS}}^{(5)}(M_Z)$ from lattice determinations in Eq. (344) with the nonlattice average from the PDG.

9.1.1 Scheme and scale dependence of α_s and $\Lambda_{\rm QCD}$

Despite the fact that the notion of the QCD coupling is initially a perturbative concept, the associated Λ parameter is nonperturbatively defined

$$\Lambda \equiv \mu \, (b_0 \bar{g}_s^2(\mu))^{-b_1/(2b_0^2)} e^{-1/(2b_0 \bar{g}_s^2(\mu))} \exp\left[-\int_0^{\bar{g}_s(\mu)} dx \left(\frac{1}{\beta(x)} + \frac{1}{b_0 x^3} - \frac{b_1}{b_0^2 x}\right)\right], \tag{282}$$

where β is the full renormalization group function in the scheme which defines $\bar{g}_s$, and b_0 and b_1 are the first two scheme-independent coefficients of the perturbative expansion

$$\beta(x) \sim -b_0 x^3 - b_1 x^5 + \dots, \tag{283}$$

with

$$b_0 = \frac{1}{(4\pi)^2}\left(11 - \frac{2}{3}N_f\right), \qquad b_1 = \frac{1}{(4\pi)^4}\left(102 - \frac{38}{3}N_f\right). \tag{284}$$

Thus the Λ parameter is renormalization-scheme-dependent but in an exactly computable way, and lattice gauge theory is an ideal method to relate it to the low-energy properties of QCD. In the $\overline{\rm MS}$ scheme presently b_{n_l} with $n_l = 4$ is known.

The change in the coupling from one scheme S to another (taken here to be the $\overline{\text{MS}}$ scheme) is perturbative,

$$g_{\overline{\text{MS}}}^2(\mu) = g_{\text{S}}^2(\mu)(1 + c_g^{(1)} g_{\text{S}}^2(\mu) + \dots), \tag{285}$$

where $c_g^{(i)}$, $i \geq 1$ are finite renormalization coefficients. The scale μ must be taken high enough for the error in keeping only the first few terms in the expansion to be small. On the other hand, the conversion to the Λ parameter in the $\overline{\text{MS}}$ scheme is given exactly by

$$\Lambda_{\overline{\text{MS}}} = \Lambda_{\text{S}} \exp\left[c_g^{(1)}/(2b_0)\right]. \tag{286}$$

The fact that $\Lambda_{\overline{\text{MS}}}$ can be obtained exactly from Λ_S in any scheme S where $c_g^{(1)}$ is known together with the high order knowledge (5-loop by now) of $\beta_{\overline{\text{MS}}}$ means that the errors in $\alpha_{\overline{\text{MS}}}(m_Z)$ are dominantly due to the errors of Λ_S. We will therefore mostly discuss them in that way. Starting from Eq. (280), we have to consider (i) the error of $\bar{g}_S^2(\mu)$ (denoted as $\left(\frac{\Delta\Lambda}{\Lambda}\right)_{\Delta\alpha_S}$) and (ii) the truncation error in β_S (denoted as $\left(\frac{\Delta\Lambda}{\Lambda}\right)_{\text{trunc}}$). Concerning (ii), note that knowledge of $c_g^{(n_l)}$ for the scheme S means that β_S is known to $n_l + 1$ loop order; b_{n_l} is known. We thus see that in the region where perturbation theory can be applied, the following errors of Λ_S (or consequently $\Lambda_{\overline{\text{MS}}}$) have to be considered

$$\left(\frac{\Delta\Lambda}{\Lambda}\right)_{\Delta\alpha_S} = \frac{\Delta\alpha_S(\mu)}{8\pi b_0 \alpha_S^2(\mu)} \times [1 + \text{O}(\alpha_S(\mu))], \tag{287}$$

$$\left(\frac{\Delta\Lambda}{\Lambda}\right)_{\text{trunc}} = k\alpha_S^{n_l}(\mu) + \text{O}(\alpha_S^{n_l+1}(\mu)), \tag{288}$$

where k is proportional to b_{n_l+1} and in typical good schemes such as $\overline{\text{MS}}$ it is numerically of order one. Statistical and systematic errors such as discretization effects contribute to $\Delta\alpha_S(\mu)$. In the above we dropped a scheme subscript for the Λ-parameters because of Eq. (284).

By convention $\alpha_{\overline{\text{MS}}}$ is usually quoted at a scale $\mu = M_Z$ where the appropriate effective coupling is the one in the 5-flavour theory: $\alpha_{\overline{\text{MS}}}^{(5)}(M_Z)$. In order to obtain it from a result with fewer flavours, one connects effective theories with different number of flavours as discussed by Bernreuther and Wetzel [12]. For example, one considers the $\overline{\text{MS}}$ scheme, matches the 3-flavour theory to the 4-flavour theory at a scale given by the charm-quark mass [13–15], runs with the 5-loop β-function [16–20] of the 4-flavour theory to a scale given by the b-quark mass, and there matches to the 5-flavour theory, after which one runs up to $\mu = M_Z$ with the 5-loop β function. For the matching relation at a given quark threshold we use the mass $m_\star$ which satisfies $m_\star = \overline{m}_{\overline{\text{MS}}}(m_\star)$, where $\overline{m}$ is the running mass (analogous to the running coupling). Then

$$\bar{g}_{N_f-1}^2(m_\star) = \bar{g}_{N_f}^2(m_\star) \times \left[1 + 0 \times \bar{g}_{N_f}^2(m_\star) + \sum_{n\geq 2} t_n \bar{g}_{N_f}^{2n}(m_\star)\right] \tag{289}$$

with [13, 15, 21]

$$t_2 = \frac{1}{(4\pi^2)^2}\frac{11}{72}, \tag{290}$$

$$t_3 = \frac{1}{(4\pi^2)^3}\left[-\frac{82043}{27648}\zeta_3 + \frac{564731}{124416} - \frac{2633}{31104}(N_f - 1)\right], \tag{291}$$

$$t_4 = \frac{1}{(4\pi^2)^4}\left[5.170347 - 1.009932(N_f - 1) - 0.021978\,(N_f - 1)^2\right], \tag{292}$$

(where ζ_3 is the Riemann zeta-function) provides the matching at the thresholds in the $\overline{\text{MS}}$ scheme. Often the package `RunDec` is used for quark-threshold matching and running in the $\overline{\text{MS}}$-scheme [22, 23].

While t_2, t_3, t_4 are numerically small coefficients, the charm threshold scale is also relatively low and so there are nonperturbative uncertainties in the matching procedure, which are difficult to estimate but which we assume here to be negligible. Obviously there is no perturbative matching formula across the strange "threshold"; here matching is entirely nonperturbative. Model dependent extrapolations of $\bar{g}^2_{N_f}$ from $N_f = 0, 2$ to $N_f = 3$ were done in the early days of lattice gauge theory. We will include these in our listings of results but not in our estimates, since such extrapolations are based on untestable assumptions.

9.1.2 Overview of the review of α_s

We begin by explaining lattice-specific difficulties in Sec. 9.2.1 and the FLAG criteria designed to assess whether the associated systematic uncertainties can be controlled and estimated in a reasonable manner. We then discuss, in Sec. 9.3 – Sec. 9.8, the various lattice approaches. For completeness, we present results from calculations with $N_f = 0, 2, 3$, and 4 flavours. Finally, in Sec. 9.10, we present averages together with our best estimates for $\alpha^{(5)}_{\overline{\text{MS}}}$. These are determined from 3- and 4-flavour QCD simulations. The earlier $N_f = 0, 2$ works obtained results for $N_f = 3$ by extrapolation in N_f. Because this is not a theoretically controlled procedure, we do not include these results in our averages. For the Λ parameter, we also give results for other number of flavours, including $N_f = 0$. Even though the latter numbers should not be used for phenomenology, they represent valuable nonperturbative information concerning field theories with variable numbers of quarks.

9.1.3 Additions with respect to the FLAG 13 report

Computations added in FLAG 16 were

Karbstein 14 [24] and Bazavov 14 [25] based on the static-quark potential (Sec. 9.4),

FlowQCD 15 [26] based on a tadpole-improved bare coupling (Sec. 9.6),

HPQCD 14A [27] based on heavy-quark current two-point functions (Sec. 9.7).

They influenced the final ranges marginally.

9.1.4 Additions with respect to the FLAG 16 report

For the benefit of the readers who are familiar with our previous report, we list here where changes and additions can be found which go beyond slight improvements of the presentation.

Our criteria are slightly updated, keeping up-to-date with the cited precisions of computations. In particular, in the criterion for perturbative behaviour we specify that the requirement may be less stringent if a larger uncertainty is quoted.

The FLAG 19 additions are

ALPHA 17 [28] and Ishikawa 17 [29] from step-scaling methods (Sec. 9.3).

Husung 17 [30], Karbstein 18 [31] and Takaura 18 [32, 33] from the static-quark potential (Sec. 9.4).

Hudspith 18 [34] based on the vacuum polarization (Sec. 9.5).

Kitazawa 16 [35] based on a tadpole-improved bare coupling (Sec. 9.6).

JLQCD 16 [36] and Maezawa 16 [37] based on heavy-quark current two-point functions (Sec. 9.7).

Nakayama 18 [38] from the eigenvalue spectrum of the Dirac operator (Sec. 9.9).

9.2   General issues

9.2.1   Discussion of criteria for computations entering the averages

As in the PDG review, we only use calculations of α_s published in peer-reviewed journals, and that use NNLO or higher-order perturbative expansions, to obtain our final range in Sec. 9.10. We also, however, introduce further criteria designed to assess the ability to control important systematics, which we describe here. Some of these criteria, e.g., that for the continuum extrapolation, are associated with lattice-specific systematics and have no continuum analogue. Other criteria, e.g., that for the renormalization scale, could in principle be applied to nonlattice determinations. Expecting that lattice calculations will continue to improve significantly in the near future, our goal in reviewing the state of the art here is to be conservative and avoid prematurely choosing an overly small range.

In lattice calculations, we generally take $\mathcal{Q}$ to be some combination of physical amplitudes or Euclidean correlation functions which are free from UV and IR divergences and have a well-defined continuum limit. Examples include the force between static quarks and two-point functions of quark bilinear currents.

In comparison to values of observables $\mathcal{Q}$ determined experimentally, those from lattice calculations require two more steps. The first step concerns setting the scale μ in GeV, where one needs to use some experimentally measurable low-energy scale as input. Ideally one employs a hadron mass. Alternatively convenient intermediate scales such as $\sqrt{t_0}$, w_0, r_0, r_1, [39–42] can be used if their relation to an experimental dimensionful observable is established. The low-energy scale needs to be computed at the same bare parameters where $\mathcal{Q}$ is determined, at least as long as one does not use the step-scaling method (see below). This induces a practical difficulty given present computing resources. In the determination of the low-energy reference scale the volume needs to be large enough to avoid finite-size effects. On the other hand, in order for the perturbative expansion of Eq. (278) to be reliable, one has to reach sufficiently high values of μ, i.e., short enough distances. To avoid uncontrollable discretization effects the lattice spacing a has to be accordingly small. This means

$$L \gg \text{hadron size} \sim \Lambda_{\text{QCD}}^{-1} \quad \text{and} \quad 1/a \gg \mu \, , \tag{293}$$

(where L is the box size) and therefore

$$L/a \ggg \mu/\Lambda_{\text{QCD}} \, . \tag{294}$$

The currently available computer power, however, limits L/a, typically to $L/a = 32 - 96$. Unless one accepts compromises in controlling discretization errors or finite-size effects, this means one needs to set the scale μ according to

$$\mu \lll L/a \times \Lambda_{\text{QCD}} \quad \sim 10 - 30 \, \text{GeV} \, . \tag{295}$$

(Here $\lll$ or $\ggg$ means at least one order of magnitude smaller or larger.) Therefore, μ can be $1-3\,\mathrm{GeV}$ at most. This raises the concern whether the asymptotic perturbative expansion truncated at 1-loop, 2-loop, or 3-loop in Eq. (278) is sufficiently accurate. There is a finite-size scaling method, usually called step-scaling method, which solves this problem by identifying $\mu = 1/L$ in the definition of $\mathcal{Q}(\mu)$, see Sec. 9.3.

For the second step after setting the scale μ in physical units (GeV), one should compute $\mathcal{Q}$ on the lattice, $\mathcal{Q}_{\mathrm{lat}}(a, \mu)$ for several lattice spacings and take the continuum limit to obtain the left hand side of Eq. (278) as

$$\mathcal{Q}(\mu) \equiv \lim_{a \to 0} \mathcal{Q}_{\mathrm{lat}}(a, \mu) \text{ with } \mu \text{ fixed}. \tag{296}$$

This is necessary to remove the discretization error.

Here it is assumed that the quantity $\mathcal{Q}$ has a continuum limit, which is regularization-independent. The method discussed in Sec. 9.6, which is based on the perturbative expansion of a lattice-regulated, divergent short-distance quantity $W_{\mathrm{lat}}(a)$ differs in this respect and must be treated separately.

In summary, a controlled determination of α_s needs to satisfy the following:

1. The determination of α_s is based on a comparison of a short-distance quantity $\mathcal{Q}$ at scale μ with a well-defined continuum limit without UV and IR divergences to a perturbative expansion formula in Eq. (278).

2. The scale μ is large enough so that the perturbative expansion in Eq. (278) is precise to the order at which it is truncated, i.e., it has good *asymptotic* convergence.

3. If $\mathcal{Q}$ is defined by physical quantities in infinite volume, one needs to satisfy Eq. (292).

Nonuniversal quantities need a separate discussion, see Sec. 9.6.

Conditions 2. and 3. give approximate lower and upper bounds for μ respectively. It is important to see whether there is a window to satisfy 2. and 3. at the same time. If it exists, it remains to examine whether a particular lattice calculation is done inside the window or not.

Obviously, an important issue for the reliability of a calculation is whether the scale μ that can be reached lies in a regime where perturbation theory can be applied with confidence. However, the value of μ does not provide an unambiguous criterion. For instance, the Schrödinger Functional, or SF-coupling (Sec. 9.3) is conventionally taken at the scale $\mu = 1/L$, but one could also choose $\mu = 2/L$. Instead of μ we therefore define an effective α_{eff}. For schemes such as SF (see Sec. 9.3) or qq (see Sec. 9.4) this is directly the coupling of the scheme. For other schemes such as the vacuum polarization we use the perturbative expansion Eq. (278) for the observable $\mathcal{Q}$ to define

$$\alpha_{\mathrm{eff}} = \mathcal{Q}/c_1. \tag{297}$$

If there is an α_s-independent term it should first be subtracted. Note that this is nothing but defining an effective, regularization-independent coupling, a physical renormalization scheme.

Let us now comment further on the use of the perturbative series. Since it is only an asymptotic expansion, the remainder $R_n(\mathcal{Q}) = \mathcal{Q} - \sum_{i \leq n} c_i \alpha_s^i$ of a truncated perturbative expression $\mathcal{Q} \sim \sum_{i \leq n} c_i \alpha_s^i$ cannot just be estimated as a perturbative error $k\,\alpha_s^{n+1}$. The error

is nonperturbative. Often one speaks of "nonperturbative contributions", but nonperturbative and perturbative cannot be strictly separated due to the asymptotic nature of the series (see, e.g., Ref. [43]).

Still, we do have some general ideas concerning the size of nonperturbative effects. The known ones such as instantons or renormalons decay for large μ like inverse powers of μ and are thus roughly of the form

$$\exp(-\gamma/\alpha_s)\,, \tag{298}$$

with some positive constant γ. Thus we have, loosely speaking,

$$\mathcal{Q} = c_1\alpha_s + c_2\alpha_s^2 + \ldots + c_n\alpha_s^n + \mathcal{O}(\alpha_s^{n+1}) + \mathcal{O}(\exp(-\gamma/\alpha_s))\,. \tag{299}$$

For small α_s, the $\exp(-\gamma/\alpha_s)$ is negligible. Similarly the perturbative estimate for the magnitude of relative errors in Eq. (297) is small; as an illustration for $n = 3$ and $\alpha_s = 0.2$ the relative error is $\sim 0.8\%$ (assuming coefficients $|c_{n+1}/c_1| \sim 1$).

For larger values of α_s nonperturbative effects can become significant in Eq. (297). An instructive example comes from the values obtained from τ decays, for which $\alpha_s \approx 0.3$. Here, different applications of perturbation theory (fixed order and contour improved) each look reasonably asymptotically convergent but the difference does not seem to decrease much with the order (see, e.g., the contribution of Pich in Ref. [44]). In addition nonperturbative terms in the spectral function may be nonnegligible even after the integration up to m_τ (see, e.g., Refs. [45], [46]). All of this is because α_s is not really small.

Since the size of the nonperturbative effects is very hard to estimate one should try to avoid such regions of the coupling. In a fully controlled computation one would like to verify the perturbative behaviour by changing α_s over a significant range instead of estimating the errors as $\sim \alpha_s^{n+1}$. Some computations try to take nonperturbative power 'corrections' to the perturbative series into account by including such terms in a fit to the μ-dependence. We note that this is a delicate procedure, both because the separation of nonperturbative and perturbative is theoretically not well defined and because in practice a term like, e.g., $\alpha_s(\mu)^3$ is hard to distinguish from a $1/\mu^2$ term when the μ-range is restricted and statistical and systematic errors are present. We consider it safer to restrict the fit range to the region where the power corrections are negligible compared to the estimated perturbative error.

The above considerations lead us to the following special criteria for the determination of α_s:

- Renormalization scale

    - ★ all points relevant in the analysis have $\alpha_{\text{eff}} < 0.2$
    - ○ all points have $\alpha_{\text{eff}} < 0.4$ and at least one $\alpha_{\text{eff}} \leq 0.25$
    - ■ otherwise

- Perturbative behaviour

    - ★ verified over a range of a factor 4 change in $\alpha_{\text{eff}}^{n_1}$ without power corrections or alternatively $\alpha_{\text{eff}}^{n_1} \leq \frac{1}{2}\Delta\alpha_{\text{eff}}/(8\pi b_0\alpha_{\text{eff}}^2)$ is reached
    - ○ agreement with perturbation theory over a range of a factor $(3/2)^2$ in $\alpha_{\text{eff}}^{n_1}$ possibly fitting with power corrections or alternatively $\alpha_{\text{eff}}^{n_1} \leq \Delta\alpha_{\text{eff}}/(8\pi b_0\alpha_{\text{eff}}^2)$ is reached

■ otherwise

Here $\Delta\alpha_{\text{eff}}$ is the accuracy cited for the determination of α_{eff} and n_{l} is the loop order to which the connection of α_{eff} to the $\overline{\text{MS}}$ scheme is known. Recall the discussion around Eqs. (285,286) The β-function of α_{eff} is then known to $n_{\text{l}} + 1$ loop order.[1]

- Continuum extrapolation

  At a reference point of $\alpha_{\text{eff}} = 0.3$ (or less) we require

  ★ three lattice spacings with $\mu a < 1/2$ and full $\mathcal{O}(a)$ improvement,
  or three lattice spacings with $\mu a \leq 1/4$ and 2-loop $\mathcal{O}(a)$ improvement,
  or $\mu a \leq 1/8$ and 1-loop $\mathcal{O}(a)$ improvement

  ○ three lattice spacings with $\mu a < 3/2$ reaching down to $\mu a = 1$ and full $\mathcal{O}(a)$ improvement,
  or three lattice spacings with $\mu a \leq 1/4$ and 1-loop $\mathcal{O}(a)$ improvement

  ■ otherwise

We also need to specify what is meant by μ. Here are our choices:

$$
\begin{aligned}
\text{step-scaling} &: \quad \mu = 1/L\,, \\
\text{heavy quark-antiquark potential} &: \quad \mu = 2/r\,, \\
\text{observables in momentum space} &: \quad \mu = q\,, \\
\text{moments of heavy-quark currents} &: \quad \mu = 2\bar{m}_{\text{c}}\,, \\
\text{eigenvalues of the Dirac operator} &: \quad \mu = \lambda_{\overline{\text{MS}}}
\end{aligned}
\tag{300}
$$

where q is the magnitude of the momentum, $\bar{m}_{\text{c}}$ the heavy-quark mass, usually taken around the charm quark mass and $\lambda_{\overline{\text{MS}}}$ is the eigenvalue of the Dirac operator, see Sec. 9.9. We note again that the above criteria cannot be applied when regularization dependent quantities $W_{\text{lat}}(a)$ are used instead of $\mathcal{O}(\mu)$. These cases are specifically discussed in Sec. 9.6.

In principle one should also account for electro-weak radiative corrections. However, both in the determination of α_s at intermediate scales μ and in the running to high scales, we expect electro-weak effects to be much smaller than the presently reached precision. Such effects are therefore not further discussed.

The attentive reader will have noticed that bounds such as $\mu a < 3/2$ or at least one value of $\alpha_{\text{eff}} \leq 0.25$ which we require for a ○ are not very stringent. There is a considerable difference between ○ and ★. We have chosen the above bounds, unchanged as compared to FLAG 16, since not too many computations would satisfy more stringent ones at present. Nevertheless, we believe that the ○ criteria already give reasonable bases for estimates of systematic errors. In the future, we expect that we will be able to tighten our criteria for inclusion in the average, and that many more computations will reach the present ★ rating in one or more categories.

---

[1]Once one is in the perturbative region with α_{eff}, the error in extracting the Λ parameter due to the truncation of perturbation theory scales like $\alpha_{\text{eff}}^{n_{\text{l}}}$, as discussed around Eq. (286). In order to detect/control such corrections properly, one needs to change the correction term significantly; we require a factor of four for a ★ and a factor $(3/2)^2$ for a ○. An exception to the above is the situation where the correction terms are small anyway, i.e., $\alpha_{\text{eff}}^{n_{\text{l}}} = \Delta\Lambda/\Lambda \approx \Delta\alpha_{\text{eff}}/(8\pi b_0 \alpha_{\text{eff}}^2)$ is reached.

In addition to our explicit criteria, the following effects may influence the precision of results:

Topology sampling: In principle a good way to improve the quality of determinations of α_s is to push to very small lattice spacings thus enabling large μ. It is known that the sampling of field space becomes very difficult for the HMC algorithm when the lattice spacing is small and one has the standard periodic boundary conditions. In practice, for all known discretizations the topological charge slows down dramatically for $a \approx 0.05$ fm and smaller [47–53]. Open boundary conditions solve the problem [54] but are not frequently used. Since the effect of the freezing on short distance observables is not known, we also do need to pay attention to this issue. Remarks are added in the text when appropriate.

Quark-mass effects: We assume that effects of the finite masses of the light quarks (including strange) are negligible in the effective coupling itself where large, perturbative, μ is considered.

Scale determination: The scale does not need to be very precise, since using the lowest-order β-function shows that a 3% error in the scale determination corresponds to a $\sim 0.5\%$ error in $\alpha_s(M_Z)$. So as long as systematic errors from chiral extrapolation and finite-volume effects are well below 3% we do not need to be concerned about those at the present level of precision in $\alpha_s(M_Z)$. This may change in the future.

9.2.2 Physical scale

A popular scale choice has been the intermediate r_0 scale. One should bear in mind that its determination from physical observables also has to be taken into account. The phenomenological value of r_0 was originally determined as $r_0 \approx 0.49$ fm through potential models describing quarkonia [41]. Of course the quantity is precisely defined, independent of such model considerations. But a lattice computation with the correct sea-quark content is needed to determine a completely sharp value. When the quark content is not quite realistic, the value of r_0 may depend to some extent on which experimental input is used to determine (actually define) it.

The latest determinations from two-flavour QCD are $r_0 = 0.420(14)$–$0.450(14)$ fm by the ETM collaboration [55, 56], using as input f_π and f_K and carrying out various continuum extrapolations. On the other hand, the ALPHA collaboration [57] determined $r_0 = 0.503(10)$ fm with input from f_K, and the QCDSF collaboration [58] cites $0.501(10)(11)$ fm from the mass of the nucleon (no continuum limit). Recent determinations from three-flavour QCD are consistent with $r_1 = 0.313(3)$ fm and $r_0 = 0.472(5)$ fm [59–61]. Due to the uncertainty in these estimates, and as many results are based directly on r_0 to set the scale, we shall often give both the dimensionless number $r_0\Lambda_{\overline{\text{MS}}}$, as well as $\Lambda_{\overline{\text{MS}}}$. In the cases where no physical r_0 scale is given in the original papers or we convert to the r_0 scale, we use the value $r_0 = 0.472$ fm. In case $r_1\Lambda_{\overline{\text{MS}}}$ is given in the publications, we use $r_0/r_1 = 1.508$ [61], to convert, which remains well consistent with the update [52] neglecting the error on this ratio. In some, mostly early, computations the string tension, $\sqrt{\sigma}$ was used. We convert to r_0 using $r_0^2\sigma = 1.65 - \pi/12$, which has been shown to be an excellent approximation in the relevant pure gauge theory [62, 63].

The new scales t_0, w_0 based on the gradient flow are very attractive alternatives to r_0 but their discretization errors are still under discussion [64–67] and their values at the physical point are not yet determined with great precision. We remain with r_0 as our main reference scale for now. A general discussion of the various scales is given in [68].

9.2.3 Studies of truncation errors of perturbation theory

As discussed previously, we have to determine α_s in a region where the perturbative expansion for the β-function, Eq. (281) in the integral Eq. (280), is reliable. In principle this must be checked, however this is difficult to achieve as we need to reach up to a sufficiently high scale. A frequently used recipe to estimate the size of truncation errors of the perturbative series is to vary the renormalization-scale dependence around the chosen 'optimal' scale μ_*, of an observable evaluated at a fixed order in the coupling from $\mu = \mu_*/2$ to $2\mu_*$. For an example see Fig. 35. Alternatively, or in addition, the renormalization scheme chosen can be varied, which investigates the perturbative conversion of the chosen scheme to the perturbatively defined $\overline{\text{MS}}$ scheme and in particular 'fastest apparent convergence' when the 'optimal' scale is chosen so that the $O(\alpha_s^2)$ coefficient vanishes.

The ALPHA collaboration in Ref. [69] and ALPHA 17 [70], within the SF approach defined a set of ν schemes where the third scheme-dependent coefficient of the β-function for $N_f = 2 + 1$ flavours was computed to be $b_2^\nu = -(0.064(27) + 1.259(1)\nu)/(4\pi)^3$. The standard SF scheme has $\nu = 0$. For comparison, $b_2^{\overline{\text{MS}}} = 0.324/(4\pi)^3$. A range of scales from about $4\,\text{GeV}$ to $128\,\text{GeV}$ was investigated. It was found that while the procedure of varying the scale by a factor 2 up and down gave a correct estimate of the residual perturbative error for $\nu \approx 0\dots0.3$, for negative values, e.g., $\nu = -0.5$, the estimated perturbative error is much too small to account for the mismatch in the Λ-parameter of $\approx 8\%$ at $\alpha_s = 0.15$. This mismatch, however, did, as expected, still scale with $\alpha_s^{n_l}$ with $n_l = 2$. In the schemes with negative ν, the coupling α_s has to be quite small for scale-variations of a factor 2 to correctly signal the perturbative errors.

A similar $\approx 8\%$ deviation in the Λ-parameter extracted from the qq-scheme (c.f. Sec. 9.4) is found by Husung 17 [30], but at $\alpha_s \approx 0.2$ and with $n_l = 3$.

9.3 α_s from Step-Scaling Methods

9.3.1 General considerations

The method of step-scaling functions avoids the scale problem, Eq. (291). It is in principle independent of the particular boundary conditions used and was first developed with periodic boundary conditions in a two-dimensional model [71].

The essential idea of the step-scaling strategy is to split the determination of the running coupling at large μ and of a hadronic scale into two lattice calculations and connect them by 'step-scaling'. In the former part, we determine the running coupling constant in a finite-volume scheme in which the renormalization scale is set by the inverse lattice size $\mu = 1/L$. In this calculation, one takes a high renormalization scale while keeping the lattice spacing sufficiently small as

$$\mu \equiv 1/L \sim 10 \dots 100\,\text{GeV}\,, \qquad a/L \ll 1\,. \tag{301}$$

In the latter part, one chooses a certain $\bar{g}_{\text{max}}^2 = \bar{g}^2(1/L_{\text{max}})$, typically such that L_{max} is around 0.5–1 fm. With a common discretization, one then determines L_{max}/a and (in a large volume $L \geq 2$–3 fm) a hadronic scale such as a hadron mass, $\sqrt{t_0}/a$ or r_0/a at the same bare parameters. In this way one gets numbers for, e.g., L_{max}/r_0 and by changing the lattice spacing a carries out a continuum limit extrapolation of that ratio.

In order to connect $\bar{g}^2(1/L_{\text{max}})$ to $\bar{g}^2(\mu)$ at high μ, one determines the change of the coupling in the continuum limit when the scale changes from L to L/s, starting from $L = L_{\text{max}}$

and arriving at $\mu = s^k/L_{\max}$. This part of the strategy is called step-scaling. Combining these results yields $\bar{g}^2(\mu)$ at $\mu = s^k\,(r_0/L_{\max})\,r_0^{-1}$, where r_0 stands for the particular chosen hadronic scale. Most applications use a scale factor $s = 2$.

At present most applications in QCD use Schrödinger functional boundary conditions [72, 73] and we discuss this below in a little more detail. (However, other boundary conditions are also possible, such as twisted boundary conditions and the discussion also applies to them.) An important reason is that these boundary conditions avoid zero modes for the quark fields and quartic modes [74] in the perturbative expansion in the gauge fields. Furthermore the corresponding renormalization scheme is well studied in perturbation theory [75–77] with the 3-loop β-function and 2-loop cutoff effects (for the standard Wilson regularization) known.

In order to have a perturbatively well-defined scheme, the SF scheme uses Dirichlet boundary conditions at time $t = 0$ and $t = T$. These break translation invariance and permit $\mathcal{O}(a)$ counter terms at the boundary through quantum corrections. Therefore, the leading discretization error is $\mathcal{O}(a)$. Improving the lattice action is achieved by adding counter terms at the boundaries whose coefficients are denoted as $c_t, \tilde{c}_t$. In practice, these coefficients are computed with 1-loop or 2-loop perturbative accuracy. A better precision in this step yields a better control over discretization errors, which is important, as can be seen, e.g., in Refs. [62, 78].

Also computations with Dirichlet boundary conditions do in principle suffer from the insufficient change of topology in the HMC algorithm at small lattice spacing. However, in a small volume the weight of nonzero charge sectors in the path integral is exponentially suppressed [79] [2] and in a Monte Carlo run of typical length very few configurations with nontrivial topology should appear. Considering the issue quantitatively Ref. [80] finds a strong suppression below $L \approx 0.8$ fm. Therefore the lack of topology change of the HMC is not a serious issue. Still Ref. [81] includes a projection to zero topology into the *definition* of the coupling. We note also that a mix of Dirichlet and open boundary conditions is expected to remove the topology issue entirely [82] and may be considered in the future.

Apart from the boundary conditions, the very definition of the coupling needs to be chosen. We briefly discuss in turn, the two schemes used at present, namely, the 'Schrödinger Functional' (SF) and 'Gradient Flow' (GF) schemes.

The SF scheme is the first one, which was used in step-scaling studies in gauge theories [72]. Inhomogeneous Dirichlet boundary conditions are imposed in time,

$$A_k(x)|_{x_0=0} = C_k\,, \quad A_k(x)|_{x_0=L} = C_k'\,, \tag{302}$$

for $k = 1, 2, 3$. Periodic boundary conditions (up to a phase for the fermion fields) with period L are imposed in space. The matrices

$$LC_k = i \operatorname{diag}\bigl(\eta - \pi/3, -\eta/2, -\eta/2 + \pi/3\bigr)\,,$$
$$LC_k' = i \operatorname{diag}\bigl(-(\eta + \pi), \eta/2 + \pi/3, \eta/2 + 2\pi/3\bigr)\,,$$

just depend on the dimensionless parameter η. The coupling $\bar{g}_{\mathrm{SF}}$ is obtained from the η-derivative of the effective action,

$$\langle \partial_\eta S|_{\eta=0}\rangle = \frac{12\pi}{\bar{g}_{\mathrm{SF}}^2}\,. \tag{303}$$

---

[2] We simplify here and assume that the classical solution associated with the used boundary conditions has charge zero. In practice this is the case.

For this scheme, the finite $c_g^{(i)}$, Eq. (283), are known for $i = 1, 2$ [76, 77].

More recently, gradient flow couplings have been used frequently because of their small statistical errors at large couplings (in contrast to $\bar{g}_{\text{SF}}$, which has small statistical errors at small couplings). The gradient flow is introduced as follows [39, 83]. Consider the flow gauge field $B_\mu(t, x)$ with the flow time t, which is a one parameter deformation of the bare gauge field $A_\mu(x)$, where $B_\mu(t, x)$ is the solution to the gradient flow equation

$$\begin{aligned} \partial_t B_\mu(t, x) &= D_\nu G_{\nu\mu}(t, x) \,, \\ G_{\mu\nu} &= \partial_\mu B_\nu - \partial_\nu B_\mu + [B_\mu, B_\nu] \,, \end{aligned} \tag{304}$$

with initial condition $B_\mu(0, x) = A_\mu(x)$. The renormalized coupling is defined by [39]

$$\bar{g}_{\text{GF}}^2(\mu) = \mathcal{N} t^2 \langle E(t, x) \rangle \big|_{\mu=1/\sqrt{8t}} \,, \tag{305}$$

with $\mathcal{N} = 16\pi^2/3 + O((a/L)^2)$ and where $E(t, x)$ is the action density given by

$$E(t, x) = \frac{1}{4} G_{\mu\nu}^a(t, x) G_{\mu\nu}^a(t, x). \tag{306}$$

In a finite volume, one needs to specify additional conditions. In order not to introduce two independent scales one sets

$$\sqrt{8t} = cL \,, \tag{307}$$

for some fixed number c [84]. Schrödinger functional boundary conditions [85] or twisted boundary conditions [29, 86] have been employed. Matching of the GF coupling to the $\overline{\text{MS}}$ scheme coupling is known to 1-loop for twisted boundary conditions with zero quark flavours and $SU(3)$ group [29] and to 2-loop with SF boundary conditions with zero quark flavours [87]. The former is based on a MC evaluation at small couplings and the latter on numerical stochastic perturbation theory.

9.3.2   Discussion of computations

In Tab. 53 we give results from various determinations of the Λ parameter. For a clear assessment of the N_f-dependence, the last column also shows results that refer to a common hadronic scale, r_0. As discussed above, the renormalization scale can be chosen large enough such that $\alpha_s < 0.2$ and the perturbative behaviour can be verified. Consequently only ★ is present for these criteria except for early work where the $n_l = 2$ loop connection to $\overline{\text{MS}}$ was not yet known and we assigned a ■ concerning the renormalization scale. With dynamical fermions, results for the step-scaling functions are always available for at least $a/L = \mu a = 1/4, 1/6, 1/8$. All calculations have a nonperturbatively $\mathcal{O}(a)$ improved action in the bulk. For the discussed boundary $\mathcal{O}(a)$ terms this is not so. In most recent calculations 2-loop $\mathcal{O}(a)$ improvement is employed together with at least three lattice spacings.[3] This means a ★ for the continuum extrapolation. In other computations only 1-loop c_t was available and we arrive at ○. We note that the discretization errors in the step-scaling functions of the SF coupling are usually found to be very small, at the percent level or below. However, the overall desired precision is very high as well, and the results in CP-PACS 04 [78] show that

---

[3]With 2-loop $\mathcal{O}(a)$ improvement we here mean c_t including the g_0^4 term and $\tilde{c}_t$ with the g_0^2 term. For gluonic observables such as the running coupling this is sufficient for cutoff effects being suppressed to $\mathcal{O}(g^6 a)$.

Collaboration Ref.		N_f	publication status	renormalization scale	perturbative behaviour	continuum extrapolation	scale	$\Lambda_{\overline{\mathrm{MS}}}[\,\mathrm{MeV}]$	$r_0\Lambda_{\overline{\mathrm{MS}}}$
ALPHA 10A	[88]	4	A	★	★	★	only running of α_s in Fig. 4		
Perez 10	[89]	4	C	★	★	○	only step-scaling function in Fig. 4		
ALPHA 17	[28]	2+1	A	★	★	★	$\sqrt{8t_0} = 0.415\,\mathrm{fm}$	341(12)	0.816(29)
PACS-CS 09A	[90]	2+1	A	★	★	○	m_ρ	$371(13)(8)(^{+0}_{-27})^{\#}$	$0.888(30)(18)(^{+0}_{-65})^{\dagger}$
			A	★	★	○	m_ρ	$345(59)^{\#\#}$	$0.824(141)^{\dagger}$
ALPHA 12*	[57]	2	A	★	★	★	f_{K}	310(20)	0.789(52)
ALPHA 04	[91]	2	A	■	★	★	$r_0 = 0.5\,\mathrm{fm}^{\S}$	$245(16)(16)^{\S}$	$0.62(2)(2)^{\S}$
ALPHA 01A	[92]	2	A	★	★	★	only running of α_s in Fig. 5		
Ishikawa 17	[29]	0	A	★	★	★	$r_0, [\sqrt{\sigma}]$	$253(4)(^{+13}_{-2})^{\dagger}$	$0.606(9)(^{+31}_{-5})^{+}$
CP-PACS 04$^{\&}$	[78]	0	A	★	★	○	only tables of g_{SF}^2		
ALPHA 98††	[93]	0	A	★	★	○	$r_0 = 0.5\mathrm{fm}$	238(19)	0.602(48)
Lüscher 93	[75]	0	A	★	○	○	$r_0 = 0.5\mathrm{fm}$	233(23)	$0.590(60)^{\S\S}$

$^{\#}$ Result with a constant (in a) continuum extrapolation of the combination $L_{\max}m_\rho$.

† In conversion from $\Lambda_{\overline{\mathrm{MS}}}$ to $r_0\Lambda_{\overline{\mathrm{MS}}}$ and vice versa, r_0 is taken to be 0.472 fm.

$^{\#\#}$ Result with a linear continuum extrapolation in a of the combination $L_{\max}m_\rho$.

* Supersedes ALPHA 04.

§ The $N_f = 2$ results were based on values for r_0/a which have later been found to be too small by [57]. The effect will be of the order of 10–15%, presumably an increase in Λr_0. We have taken this into account by a ■ in the renormalization scale.

$^{\&}$ This investigation was a precursor for PACS-CS 09A and confirmed two step-scaling functions as well as the scale setting of ALPHA 98.

†† Uses data of Lüscher 93 and therefore supersedes it.

§§ Converted from $\alpha_{\overline{\mathrm{MS}}}(37r_0^{-1}) = 0.1108(25)$.

$^{+}$ Also $\Lambda_{\overline{\mathrm{MS}}}/\sqrt{\sigma} = 0.532(8)(^{+27}_{-5})$ is quoted.

Table 53: Results for the Λ parameter from computations using step-scaling of the SF-coupling. Entries without values for Λ computed the running and established perturbative behaviour at large μ.

discretization errors at the below percent level cannot be taken for granted. In particular with staggered fermions (unimproved except for boundary terms) few percent effects are seen in Perez 10 [89].

In the work by PACS-CS 09A [90], the continuum extrapolation in the scale setting is performed using a constant function in a and with a linear function. Potentially the former leaves a considerable residual discretization error. We here use, as discussed with the collaboration, the continuum extrapolation linear in a, as given in the second line of PACS-CS

09A [90] results in Tab. 53. After perturbative conversion from a three-flavour result to five flavours (see Sec. 9.2.1), they obtain

$$\alpha_{\overline{\mathrm{MS}}}^{(5)}(M_Z) = 0.118(3)\,. \tag{308}$$

In Ref. [28], the ALPHA collaboration determined $\Lambda_{\overline{\mathrm{MS}}}^{(3)}$ combining step-scaling in $\bar{g}_{\mathrm{GF}}^2$ in the lower scale region $\mu_{\mathrm{had}} \leq \mu \leq \mu_0$, and step-scaling in $\bar{g}_{\mathrm{SF}}^2$ for higher scales $\mu_0 \leq \mu \leq \mu_{\mathrm{PT}}$. Both schemes are defined with SF boundary conditions. For $\bar{g}_{\mathrm{GF}}^2$ a projection to the sector of zero topological charge is included, Eq. (304) is restricted to the magnetic components, and $c = 0.3$. The scales μ_{had}, μ_0, and μ_{PT} are defined by $\bar{g}_{\mathrm{GF}}^2(\mu_{\mathrm{had}}) = 11.3$, $\bar{g}_{\mathrm{SF}}^2(\mu_0) = 2.012$, and $\mu_{\mathrm{PT}} = 16\mu_0$ which are roughly estimated as

$$1/L_{\max} \equiv \mu_{\mathrm{had}} \approx 0.2 \text{ GeV}\,, \quad \mu_0 \approx 4 \text{ GeV}\,, \quad \mu_{\mathrm{PT}} \approx 70 \text{ GeV}\,. \tag{309}$$

Step-scaling is carried out with an $O(a)$-improved Wilson quark action [94] and Lüscher-Weisz gauge action [95] in the low-scale region and an $O(a)$-improved Wilson quark action [96] and Wilson gauge action in the high-energy part. For the step-scaling using steps of $L/a \to 2L/a$, three lattice sizes $L/a = 8, 12, 16$ were simulated for $\bar{g}_{\mathrm{GF}}^2$ and four lattice sizes $L/a = (4,)\,6, 8, 12$ for $\bar{g}_{\mathrm{SF}}^2$. The final results do not use the small lattices given in parenthesis. The parameter $\Lambda_{\overline{\mathrm{MS}}}^{(3)}$ is then obtained via

$$\Lambda_{\overline{\mathrm{MS}}}^{(3)} = \underbrace{\frac{\Lambda_{\overline{\mathrm{MS}}}^{(3)}}{\mu_{\mathrm{PT}}}}_{\text{perturbation theory}} \times \underbrace{\frac{\mu_{\mathrm{PT}}}{\mu_{\mathrm{had}}}}_{\text{step−scaling}} \times \underbrace{\frac{\mu_{\mathrm{had}}}{f_{\pi K}}}_{\text{large volume simulation}} \times \underbrace{f_{\pi K}}_{\text{experimental data}}\,, \tag{310}$$

where the hadronic scale $f_{\pi K}$ is $f_{\pi K} = \frac{1}{3}(2f_K + f_\pi) = 147.6(5)$ MeV. The first term on the right hand side of Eq. (308) is obtained from $\alpha_{\mathrm{SF}}(\mu_{\mathrm{PT}})$ which is the output from SF step-scaling using Eq. (280) with $\alpha_{\mathrm{SF}}(\mu_{\mathrm{PT}}) \approx 0.1$ and the 3-loop β-function and the exact conversion to the $\overline{\mathrm{MS}}$-scheme. The second term is essentially obtained from step-scaling in the GF scheme and the measurement of $\bar{g}_{\mathrm{SF}}^2(\mu_0)$ except for the trivial scaling factor of 16 in the SF running. The third term is obtained from a measurement of the hadronic quantity at large volume.

A large volume simulation is done for three lattice spacings with sufficiently large volume and reasonable control over the chiral extrapolation so that the scale determination is precise enough. The step-scaling results in both schemes satisfy renormalization criteria, perturbation theory criteria, and continuum limit criteria just as previous studies using step-scaling. So we assign green stars for these criteria.

The dependence of Λ, eq. (280) with 3-loop β-function, on α_s and on the chosen scheme is discussed in [69]. This investigation provides a warning on estimating the truncation error of perturbative series. Details are explained in Sec. 9.2.3.

The result for the Λ parameter is $\Lambda_{\overline{\mathrm{MS}}}^{(3)} = 341(12)$ MeV, where the dominant error comes from the error of $\alpha_{\mathrm{SF}}(\mu_{\mathrm{PT}})$ after step-scaling in SF scheme. Using 4-loop matching at the charm and bottom thresholds and 5-loop running one finally obtains

$$\alpha_{\overline{\mathrm{MS}}}^{(5)}(M_Z) = 0.11852(84)\,. \tag{311}$$

Several other results do not have a sufficient number of quark flavours or do not yet contain the conversion of the scale to physical units (ALPHA 10A [88], Perez 10 [89]). Thus no value for $\alpha_{\overline{\mathrm{MS}}}^{(5)}(M_Z)$ is quoted.

The computation of Ishikawa et al. [29] is based on the gradient flow coupling with twisted boundary conditions [86] (TGF coupling) in the pure gauge theory. Again they use $c = 0.3$. Step-scaling with a scale factor $s = 3/2$ is employed, covering a large range of couplings from $\alpha_s \approx 0.5$ to $\alpha_s \approx 0.1$ and taking the continuum limit through global fits to the step-scaling function on $L/a = 12, 16, 18$ lattices with between 6 and 8 parameters. Systematic errors due to variations of the fit functions are estimated. Two physical scales are considered: r_0/a is taken from [62] and σa^2 from [97] and [98]. As the ratio $\Lambda_{\rm TGF}/\Lambda_{\overline{\rm MS}}$ has not yet been computed analytically, Ref. [29] determines the 1-loop relation between $\bar{g}_{\rm SF}$ and $\bar{g}_{\rm TGF}$ from MC simulations performed in the weak coupling region and then uses the known $\Lambda_{\rm SF}/\Lambda_{\overline{\rm MS}}$. Systematic errors due to variations of the fit functions dominate the overall uncertainty.

9.4 α_s from the potential at short distances

9.4.1 General considerations

The basic method was introduced in Ref. [99] and developed in Ref. [100]. The force or potential between an infinitely massive quark and antiquark pair defines an effective coupling constant via

$$F(r) = \frac{dV(r)}{dr} = C_F \frac{\alpha_{\rm qq}(r)}{r^2} \,. \tag{312}$$

The coupling can be evaluated nonperturbatively from the potential through a numerical differentiation, see below. In perturbation theory one also defines couplings in different schemes $\alpha_{\bar{V}}, \alpha_V$ via

$$V(r) = -C_F \frac{\alpha_{\bar{V}}(r)}{r} \,, \qquad \text{or} \quad \tilde{V}(Q) = -C_F \frac{\alpha_V(Q)}{Q^2} \,, \tag{313}$$

where one fixes the unphysical constant in the potential by $\lim_{r \to \infty} V(r) = 0$ and $\tilde{V}(Q)$ is the Fourier transform of $V(r)$. Nonperturbatively, the subtraction of a constant in the potential introduces an additional renormalization constant, the value of $V(r_{\rm ref})$ at some distance $r_{\rm ref}$. Perturbatively, it is believed to entail a renormalon ambiguity. In perturbation theory, the different definitions are all simply related to each other, and their perturbative expansions are known including the α_s^4, $\alpha_s^4 \log \alpha_s$ and $\alpha_s^5 \log \alpha_s$, $\alpha_s^5 (\log \alpha_s)^2$ terms [101–108].

The potential $V(r)$ is determined from ratios of Wilson loops, $W(r, t)$, which behave as

$$\langle W(r, t) \rangle = |c_0|^2 e^{-V(r)t} + \sum_{n \neq 0} |c_n|^2 e^{-V_n(r)t} \,, \tag{314}$$

where t is taken as the temporal extension of the loop, r is the spatial one and V_n are excited-state potentials. To improve the overlap with the ground state, and to suppress the effects of excited states, t is taken large. Also various additional techniques are used, such as a variational basis of operators (spatial paths) to help in projecting out the ground state. Furthermore some lattice-discretization effects can be reduced by averaging over Wilson loops related by rotational symmetry in the continuum.

In order to reduce discretization errors it is of advantage to define the numerical derivative giving the force as

$$F(r_{\rm I}) = \frac{V(r) - V(r - a)}{a} \,, \tag{315}$$

where $r_{\rm I}$ is chosen so that at tree level the force is the continuum force. $F(r_{\rm I})$ is then a 'tree-level improved' quantity and similarly the tree-level improved potential can be defined [109].

Lattice potential results are in position space, while perturbation theory is naturally computed in momentum space at large momentum. Usually, the Fourier transform of the perturbative expansion is then matched to lattice data.

Finally, as was noted in Sec. 9.2.1, a determination of the force can also be used to determine the scales r_0, r_1, by defining them from the static force by

$$r_0^2 F(r_0) = 1.65 , \quad r_1^2 F(r_1) = 1 . \tag{316}$$

9.4.2   Discussion of computations

In Tab. 54, we list results of determinations of $r_0 \Lambda_{\overline{\rm MS}}$ (together with $\Lambda_{\overline{\rm MS}}$ using the scale determination of the authors). Since the last review, FLAG 16, there have been three new computations, Husung 17 [30], Karbstein 18 [31] and Takaura 18 [32, 33].

The first determinations in the three-colour Yang Mills theory are by UKQCD 92 [100] and Bali 92 [113] who used $\alpha_{\rm qq}$ as explained above, but not in the tree-level improved form. Rather a phenomenologically determined lattice artifact correction was subtracted from the lattice potentials. The comparison with perturbation theory was on a more qualitative level on the basis of a 2-loop β-function ($n_l = 1$) and a continuum extrapolation could not be performed as yet. A much more precise computation of $\alpha_{\rm qq}$ with continuum extrapolation was performed in Refs. [62, 109]. Satisfactory agreement with perturbation theory was found [109] but the stability of the perturbative prediction was not considered sufficient to be able to extract a Λ parameter.

In Brambilla 10 [112] the same quenched lattice results of Ref. [109] were used and a fit was performed to the continuum potential, instead of the force. Perturbation theory to $n_l = 3$ loop was used including a resummation of terms $\alpha_s^3 (\alpha_s \ln \alpha_s)^n$ and $\alpha_s^4 (\alpha_s \ln \alpha_s)^n$. Close agreement with perturbation theory was found when a renormalon subtraction was performed. Note that the renormalon subtraction introduces a second scale into the perturbative formula which is absent when the force is considered.

Bazavov 14 [25] updates Bazavov 12 [110] and modifies this procedure somewhat. They consider the perturbative expansion for the force. They set $\mu = 1/r$ to eliminate logarithms and then integrate the force to obtain an expression for the potential. The resulting integration constant is fixed by requiring the perturbative potential to be equal to the nonperturbative one exactly at a reference distance $r_{\rm ref}$ and the two are then compared at other values of r. As a further check, the force is also used directly.

For the quenched calculation Brambilla 10 [112] very small lattice spacings, $a \sim 0.025\,{\rm fm}$, were available from Ref. [109]. For ETM 11C [111], Bazavov 12 [110], Karbstein 14 [24] and Bazavov 14 [25] using dynamical fermions such small lattice spacings are not yet realized (Bazavov 14 reaches down to $a \sim 0.041\,{\rm fm}$). They all use the tree-level improved potential as described above. We note that the value of $\Lambda_{\overline{\rm MS}}$ in physical units by ETM 11C [111] is based on a value of $r_0 = 0.42$ fm. This is at least 10% smaller than the large majority of other values of r_0. Also the values of r_0/a on the finest lattices in ETM 11C [111] and r_1/a for Bazavov 14 [25] come from rather small lattices with $m_\pi L \approx 2.4$, 2.2 respectively.

Instead of the procedure discussed previously, Karbstein 14 [24] reanalyzes the data of ETM 11C [111] by first estimating the Fourier transform $\tilde{V}(p)$ of $V(r)$ and then fitting the

Collaboration	Ref.	N_f	publication status	renormalization scale	perturbative behaviour	continuum extrapolation	scale	$\Lambda_{\overline{MS}}$[MeV]	$r_0\Lambda_{\overline{MS}}$
Takaura 18	[32, 33]	2+1	P	■	○	○	$\sqrt{t_0}=0.1465(25)$fm, [a]	$334(10)(^{+20}_{-18})^b$	$0.799(51)^+$
Bazavov 14	[25]	2+1	A	○	★	○	$r_1=0.3106(17)$ fm[c]	$315(^{+18}_{-12})^d$	$0.746(^{+42}_{-27})$
Bazavov 12	[110]	2+1	A	○†	○	○#	$r_0=0.468$ fm	$295(30)^\star$	$0.70(7)^{\star\star}$
Karbstein 18	[31]	2	A	○	○	○	$r_0=0.420(14)$ fm[e]	302(16)	0.643(34)
Karbstein 14	[24]	2	A	○	○	○	$r_0=0.42$ fm	331(21)	0.692(31)
ETM 11C	[111]	2	A	○	○	○	$r_0=0.42$ fm	$315(30)^\S$	0.658(55)
Husung 17	[30]	0	C	○	★	★	$r_0=0.50$ fm	232(6)	0.590(16)
Brambilla 10	[112]	0	A	○	★	○††		$266(13)^+$	$0.637(^{+32}_{-30})^{\dagger\dagger}$
UKQCD 92	[100]	0	A	★	○++	■	$\sqrt{\sigma}=0.44$ GeV	256(20)	0.686(54)
Bali 92	[113]	0	A	★	○++	■	$\sqrt{\sigma}=0.44$ GeV	247(10)	0.661(27)

[a] Scale determined from t_0 in Ref. [40].

[b] $\alpha^{(5)}_{\overline{MS}}(M_Z) = 0.1179(7)(^{+13}_{-12})$.

[c] Determination on lattices with $m_\pi L = 2.2 - 2.6$. Scale from r_1 [52] as determined from f_π in Ref. [60].

[d] $\alpha^{(3)}_{\overline{MS}}(1.5\,\mathrm{GeV}) = 0.336(^{+12}_{-8})$, $\alpha^{(5)}_{\overline{MS}}(M_Z) = 0.1166(^{+12}_{-8})$.

[e] Scale determined from f_π, see [55].

† Since values of α_{eff} within our designated range are used, we assign a ○ despite values of α_{eff} up to $\alpha_{\mathrm{eff}} = 0.5$ being used.

Since values of $2a/r$ within our designated range are used, we assign a ○ although only values of $2a/r \geq 1.14$ are used at $\alpha_{\mathrm{eff}} = 0.3$.

⋆ Using results from Ref. [61].

⋆⋆ $\alpha^{(3)}_{\overline{MS}}(1.5\,\mathrm{GeV}) = 0.326(19)$, $\alpha^{(5)}_{\overline{MS}}(M_Z) = 0.1156(^{+21}_{-22})$.

§ Both potential and r_0/a are determined on a small ($L = 3.2r_0$) lattice.

†† Uses lattice results of Ref. [62], some of which have very small lattice spacings where according to more recent investigations a bias due to the freezing of topology may be present.

+ Our conversion using $r_0 = 0.472$ fm.

++ We give a ○ because only a NLO formula is used and the error bars are very large; our criterion does not apply well to these very early calculations.

Table 54: Short-distance potential results.

perturbative expansion of $\tilde{V}(p)$ in terms of $\alpha_{\overline{MS}}(p)$. Of course, the Fourier transform requires some modelling of the r-dependence of $V(r)$ at short and at large distances. The authors fit a linearly rising potential at large distances together with string-like corrections of order r^{-n} and define the potential at large distances by this fit.[4] Recall that for observables in momentum space we take the renormalization scale entering our criteria as $\mu = q$, Eq. (298). The analysis (as in ETM 11C [111]) is dominated by the data at the smallest lattice spacing,

---

[4]Note that at large distances, where string breaking is known to occur, this is not any more the ground state potential defined by Eq. (312).

where a controlled determination of the overall scale is difficult due to possible finite-size effects. Karbstein 18 [31] is a reanalysis of Karbstein 14 and supersedes it. Some data with a different discretization of the static quark is added (on the same configurations) and the discrete lattice results for the static potential in position space are first parameterized by a continuous function, which then allows for an analytical Fourier transformation to momentum space.

Similarly also for Takaura 18 [32, 33] the momentum space potential $\tilde{V}(Q)$ is the central object. Namely, they assume that renormalon / power law effects are absent in $\tilde{V}(Q)$ and only come in through the Fourier transformation. They provide evidence that renormalon effects (both $u = 1/2$ and $u = 3/2$) can be subtracted and arrive at a nonperturbative term $k \Lambda_{\overline{\mathrm{MS}}}^3 r^2$. Two different analysis are carried out with the final result taken from "Analysis II". Our numbers including the evaluation of the criteria refer to it. Together with the perturbative 3-loop (including the $\alpha_s^4 \log \alpha_s$ term) expression, this term is fitted to the nonperturbative results for the potential in the region $0.04\,\mathrm{fm} \leq r \leq 0.35\,\mathrm{fm}$, where $0.04\,\mathrm{fm}$ is $r = a$ on the finest lattice. The NP potential data originate from JLQCD ensembles (Symanzik improved gauge action and Möbius domain-wall quarks) at three lattice spacings with a pion mass around 300 MeV. Since at the maximal distance in the analysis we find $\alpha_{\overline{\mathrm{MS}}}(2/r) = 0.43$, the renormalization scale criterion yields a ■ . The perturbative behavior is ○ because of the high order in PT known. The continuum limit criterion yields a ○ .

One of the main issues for all these computations is whether the perturbative running of the coupling constant has been reached. While for $N_f = 0$ fermions Brambilla 10 [112] reports agreement with perturbative behavior at the smallest distances, Husung 17 (which goes to shorter distances) finds relatively large corrections beyond the 3-loop α_{qq}. For dynamical fermions, Bazavov 12 [110] and Bazavov 14 [25] report good agreement with perturbation theory after the renormalon is subtracted or eliminated.

A second issue is the coverage of configuration space in some of the simulations, which use very small lattice spacings with periodic boundary conditions. Affected are the smallest two lattice spacings of Bazavov 14 [25] where very few tunnelings of the topological charge occur [52]. With present knowledge, it also seems possible that the older data by Refs. [62, 109] used by Brambilla 10 [112] are partially obtained with (close to) frozen topology.

The recent computation Husung 17 [30], for $N_f = 0$ flavours first determines the coupling $\bar{g}_{\mathrm{qq}}^2(r,a)$ from the force and then performs a continuum extrapolation on lattices down to $a \approx 0.015\,\mathrm{fm}$, using a step-scaling method at short distances, $r/r_0 \lesssim 0.5$. Using the 4-loop β^{qq} function this allows $r_0 \Lambda_{\mathrm{qq}}$ to be estimated, which is then converted to the $\overline{\mathrm{MS}}$ scheme. $\alpha_{\mathrm{eff}} = \alpha_{\mathrm{qq}}$ ranges from ~ 0.17 to large values; we give ○ for renormalization scale and ★ for perturbative behaviour. The range $a\mu = 2a/r \approx 0.37$ - 0.14 leads to a ★ in the continuum extrapolation.

We note that the $N_f = 3$ determinations of $r_0 \Lambda_{\overline{\mathrm{MS}}}$ agree within their errors of 4-6%.

9.5 α_s from the vacuum polarization at short distances

9.5.1 General considerations

The vacuum polarization function for the flavour nonsinglet currents J_μ^a ($a = 1, 2, 3$) in the momentum representation is parameterized as

$$\langle J_\mu^a J_\nu^b \rangle = \delta^{ab}[(\delta_{\mu\nu}Q^2 - Q_\mu Q_\nu)\Pi^{(1)}(Q) - Q_\mu Q_\nu \Pi^{(0)}(Q)], \tag{317}$$

where Q_μ is a space-like momentum and $J_\mu \equiv V_\mu$ for a vector current and $J_\mu \equiv A_\mu$ for an axial-vector current. Defining $\Pi_J(Q) \equiv \Pi_J^{(0)}(Q) + \Pi_J^{(1)}(Q)$, the operator product expansion (OPE) of the vacuum polarization function $\Pi_{V+A}(Q) = \Pi_V(Q) + \Pi_A(Q)$ is given by

$$\begin{aligned}
&\Pi_{V+A}|_{\mathrm{OPE}}(Q^2, \alpha_s) \\
&= c + C_1(Q^2) + C_m^{V+A}(Q^2)\frac{\bar{m}^2(Q)}{Q^2} + \sum_{q=u,d,s} C_{\bar{q}q}^{V+A}(Q^2)\frac{\langle m_q \bar{q}q \rangle}{Q^4} \\
&\quad + C_{GG}(Q^2)\frac{\langle \alpha_s GG \rangle}{Q^4} + \mathcal{O}(Q^{-6}),
\end{aligned} \tag{318}$$

for large Q^2. The perturbative coefficient functions $C_X^{V+A}(Q^2)$ for the operators X ($X = 1$, $\bar{q}q$, GG) are given as $C_X^{V+A}(Q^2) = \sum_{i\geq 0}\left(C_X^{V+A}\right)^{(i)}\alpha_s^i(Q^2)$ and $\bar{m}$ is the running mass of the mass-degenerate up and down quarks. C_1 is known including α_s^4 in a continuum renormalization scheme such as the $\overline{\mathrm{MS}}$ scheme [114–117]. Nonperturbatively, there are terms in C_X that do not have a series expansion in α_s. For an example for the unit operator see Ref. [118]. The term c is Q-independent and divergent in the limit of infinite ultraviolet cutoff. However the Adler function defined as

$$D(Q^2) \equiv -Q^2 \frac{d\Pi(Q^2)}{dQ^2}, \tag{319}$$

is a scheme-independent finite quantity. Therefore one can determine the running coupling constant in the $\overline{\mathrm{MS}}$ scheme from the vacuum polarization function computed by a lattice-QCD simulation. In more detail, the lattice data of the vacuum polarization is fitted with the perturbative formula Eq. (316) with fit parameter $\Lambda_{\overline{\mathrm{MS}}}$ parameterizing the running coupling $\alpha_{\overline{\mathrm{MS}}}(Q^2)$.

While there is no problem in discussing the OPE at the nonperturbative level, the 'condensates' such as $\langle \alpha_s GG \rangle$ are ambiguous, since they mix with lower-dimensional operators including the unity operator. Therefore one should work in the high-Q^2 regime where power corrections are negligible within the given accuracy. Thus setting the renormalization scale as $\mu \equiv \sqrt{Q^2}$, one should seek, as always, the window $\Lambda_{\mathrm{QCD}} \ll \mu \ll a^{-1}$.

9.5.2   Discussion of computations

Results using this method are, to date, only available using overlap fermions or domain wall fermions. Since the last review, FLAG 16, there has been one new computation, Hudspith 18 [34]. These are collected in Tab. 55 for $N_f = 2$, JLQCD/TWQCD 08C [121] and for $N_f = 2 + 1$, JLQCD 10 [120] and Hudspith 18 [34].

We first discuss the results of JLQCD/TWQCD 08C [121] and JLQCD 10 [120]. The fit to Eq. (316) is done with the 4-loop relation between the running coupling and $\Lambda_{\overline{\mathrm{MS}}}$. It is found that without introducing condensate contributions, the momentum scale where the perturbative formula gives good agreement with the lattice results is very narrow, $aQ \simeq 0.8 - 1.0$. When a condensate contribution is included the perturbative formula gives good agreement with the lattice results for the extended range $aQ \simeq 0.6 - 1.0$. Since there is only a single lattice spacing $a \approx 0.11\,\mathrm{fm}$ there is a ■ for the continuum limit. The renormalization scale μ is in the range of $Q = 1.6 - 2\,\mathrm{GeV}$. Approximating $\alpha_{\mathrm{eff}} \approx \alpha_{\overline{\mathrm{MS}}}(Q)$, we estimate that $\alpha_{\mathrm{eff}} = 0.25 - 0.30$ for $N_f = 2$ and $\alpha_{\mathrm{eff}} = 0.29 - 0.33$ for $N_f = 2 + 1$. Thus we give a ○ and

Collaboration	Ref.	N_f	publication status	renormalization scale	perturbative behaviour	continuum extrapolation	scale	$\Lambda_{\overline{\mathrm{MS}}}[\,\mathrm{MeV}]$	$r_0\Lambda_{\overline{\mathrm{MS}}}$
Hudspith 18	[34]	2+1	P	○	○	■	$m_\Omega{}^\star$	337(40)	$0.806(96)^a$
Hudspith 15	[119]	2+1	C	○	○	■	$m_\Omega{}^\star$	$300(24)^+$	0.717(58)
JLQCD 10	[120]	2+1	A	■	○	■	$r_0 = 0.472\,\mathrm{fm}$	$247(5)^\dagger$	0.591(12)
JLQCD/TWQCD 08C	[121]	2	A	○	○	■	$r_0 = 0.49\,\mathrm{fm}$	$234(9)(^{+16}_{-0})$	$0.581(22)(^{+40}_{-0})$

* Determined in [122].
^{a} $\alpha^{(5)}_{\overline{\mathrm{MS}}}(M_Z) = 0.1181(27)(^{+8}_{-22})$. $\Lambda_{\overline{\mathrm{MS}}}$ determined by us from $\alpha^{(3)}_{\overline{\mathrm{MS}}}(2\,\mathrm{GeV}) = 0.2961(185)$. In conversion to $r_0\Lambda$ we used $r_0 = 0.472\,\mathrm{fm}$.
$^+$ Determined by us from $\alpha^{(3)}_{\overline{\mathrm{MS}}}(2\,\mathrm{GeV}) = 0.279(11)$. Evaluates to $\alpha^{(5)}_{\overline{\mathrm{MS}}}(M_Z) = 0.1155(18)$.
† $\alpha^{(5)}_{\overline{\mathrm{MS}}}(M_Z) = 0.1118(3)(^{+16}_{-17})$.

Table 55: Vacuum polarization results.

■ for $N_f = 2$ and $N_f = 2 + 1$, respectively, for the renormalization scale and a ■ for the perturbative behaviour.

A further investigation of this method was initiated in Hudspith 15 [119] and completed by Hudspith 18 [34] (see also [123]) based on domain wall fermion configurations at three lattice spacings, $a^{-1} = 1.78$, 2.38, 3.15 GeV, with three different light quark masses on the two coarser lattices and one on the fine lattice. An extensive discussion of condensates, using continuum finite energy sum rules was employed to estimate where their contributions might be negligible. It was found that even up to terms of $O((1/Q^2)^8)$ (a higher order than depicted in Eq. (316) but with constant coefficients) no single condensate dominates and apparent convergence was poor for low Q^2 due to cancellations between contributions of similar size with alternating signs. (See, e.g., the list given by Hudspith 15 [119].) Choosing Q^2 to be at least $\sim 3.8\,\mathrm{GeV}^2$ mitigated the problem, but then the coarest lattice had to be discarded, due to large lattice artifacts. So this gives a ■ for continuum extrapolation. With the higher Q^2 the quark-mass dependence of the results was negligible, so ensembles with different quark masses were averaged over. A range of Q^2 from $3.8 - 16\,\mathrm{GeV}^2$ gives $\alpha_{\mathrm{eff}} = 0.31 - 0.22$, so there is a ○ for the renormalization scale. The value of α^3_{eff} reaches $\Delta\alpha_{\mathrm{eff}}/(8\pi b_0\alpha_{\mathrm{eff}})$ and thus gives a ○ for perturbative behaviour. In Hudspith 15 [119] (superseded by Hudspith 18 [34]) about a 20% difference in $\Pi(Q^2)$ was seen between the two lattice lattice spacings and a result is quoted only for the smaller a.

9.6 α_s from observables at the lattice spacing scale

9.6.1 General considerations

The general method is to evaluate a short-distance quantity $\mathcal{Q}$ at the scale of the lattice spacing $\sim 1/a$ and then determine its relationship to $\alpha_{\overline{\text{MS}}}$ via a perturbative expansion.

This is epitomized by the strategy of the HPQCD collaboration [124, 125], discussed here for illustration, which computes and then fits to a variety of short-distance quantities, Y,

$$Y = \sum_{n=1}^{n_{\text{max}}} c_n \alpha_{\text{V}'}^n(q^*) \, . \tag{320}$$

The quantity Y is taken as the logarithm of small Wilson loops (including some nonplanar ones), Creutz ratios, 'tadpole-improved' Wilson loops and the tadpole-improved or 'boosted' bare coupling ($\mathcal{O}(20)$ quantities in total). The perturbative coefficients c_n (each depending on the choice of Y) are known to $n = 3$ with additional coefficients up to n_{max} being fitted numerically. The running coupling $\alpha_{\text{V}'}$ is related to α_{V} from the static-quark potential (see Sec. 9.4).[5]

The coupling constant is fixed at a scale $q^* = d/a$. The latter is chosen as the mean value of $\ln q$ with the one gluon loop as measure [126, 127]. (Thus a different result for d is found for every short-distance quantity.) A rough estimate yields $d \approx \pi$, and in general the renormalization scale is always found to lie in this region.

For example, for the Wilson loop $W_{mn} \equiv \langle W(ma, na) \rangle$ we have

$$\ln \left(\frac{W_{mn}}{u_0^{2(m+n)}} \right) = c_1 \alpha_{\text{V}'}(q^*) + c_2 \alpha_{\text{V}'}^2(q^*) + c_3 \alpha_{\text{V}'}^3(q^*) + \cdots \, , \tag{321}$$

for the tadpole-improved version, where $c_1, c_2, \ldots$ are the appropriate perturbative coefficients and $u_0 = W_{11}^{1/4}$. Substituting the nonperturbative simulation value in the left hand side, we can determine $\alpha_{\text{V}'}(q^*)$, at the scale q^*. Note that one finds empirically that perturbation theory for these tadpole-improved quantities have smaller c_n coefficients and so the series has a faster apparent convergence compared to the case without tadpole improvement.

Using the β-function in the V$'$ scheme, results can be run to a reference value, chosen as $\alpha_0 \equiv \alpha_{\text{V}'}(q_0)$, $q_0 = 7.5 \, \text{GeV}$. This is then converted perturbatively to the continuum $\overline{\text{MS}}$ scheme

$$\alpha_{\overline{\text{MS}}}(q_0) = \alpha_0 + d_1 \alpha_0^2 + d_2 \alpha_0^3 + \cdots \, , \tag{322}$$

where d_1, d_2 are known 1- and 2-loop coefficients.

Other collaborations have focused more on the bare 'boosted' coupling constant and directly determined its relationship to $\alpha_{\overline{\text{MS}}}$. Specifically, the boosted coupling is defined by

$$\alpha_{\text{P}}(1/a) = \frac{1}{4\pi} \frac{g_0^2}{u_0^4} \, , \tag{323}$$

again determined at a scale $\sim 1/a$. As discussed previously, since the plaquette expectation value in the boosted coupling contains the tadpole diagram contributions to all orders, which are dominant contributions in perturbation theory, there is an expectation that the perturbation theory using the boosted coupling has smaller perturbative coefficients [126], and hence smaller perturbative errors.

---

[5] $\alpha_{\text{V}'}$ is defined by $\Lambda_{\text{V}'} = \Lambda_{\text{V}}$ and $b_i^{\text{V}'} = b_i^{\text{V}}$ for $i = 0, 1, 2$ but $b_i^{\text{V}'} = 0$ for $i \geq 3$.

9.6.2 Continuum limit

Lattice results always come along with discretization errors, which one needs to remove by a continuum extrapolation. As mentioned previously, in this respect the present method differs in principle from those in which α_s is determined from physical observables. In the general case, the numerical results of the lattice simulations at a value of μ fixed in physical units can be extrapolated to the continuum limit, and the result can be analyzed as to whether it shows perturbative running as a function of μ in the continuum. For observables at the cutoff-scale ($q^* = d/a$), discretization effects cannot easily be separated out from perturbation theory, as the scale for the coupling comes from the lattice spacing. Therefore the restriction $a\mu \ll 1$ (the 'continuum extrapolation' criterion) is not applicable here. Discretization errors of order a^2 are, however, present. Since $a \sim \exp(-1/(2b_0 g_0^2)) \sim \exp(-1/(8\pi b_0 \alpha(q^*)))$, these errors now appear as power corrections to the perturbative running, and have to be taken into account in the study of the perturbative behaviour, which is to be verified by changing a. One thus usually fits with power corrections in this method.

In order to keep a symmetry with the 'continuum extrapolation' criterion for physical observables and to remember that discretization errors are, of course, relevant, we replace it here by one for the lattice spacings used:

- Lattice spacings

  - ★ 3 or more lattice spacings, at least 2 points below $a = 0.1\,\mathrm{fm}$
  - ○ 2 lattice spacings, at least 1 point below $a = 0.1\,\mathrm{fm}$
  - ■ otherwise

9.6.3 Discussion of computations

Note that due to $\mu \sim 1/a$ being relatively large the results easily have a ★ or ○ in the rating on renormalization scale.

The work of El-Khadra 92 [135] employs a 1-loop formula to relate $\alpha_{\overline{\mathrm{MS}}}^{(0)}(\pi/a)$ to the boosted coupling for three lattice spacings $a^{-1} = 1.15,\ 1.78,\ 2.43\,\mathrm{GeV}$. (The lattice spacing is determined from the charmonium 1S-1P splitting.) They obtain $\Lambda_{\overline{\mathrm{MS}}}^{(0)} = 234\,\mathrm{MeV}$, corresponding to $\alpha_{\mathrm{eff}} = \alpha_{\overline{\mathrm{MS}}}^{(0)}(\pi/a) \approx 0.15$–$0.2$. The work of Aoki 94 [134] calculates $\alpha_V^{(2)}$ and $\alpha_{\overline{\mathrm{MS}}}^{(2)}$ for a single lattice spacing $a^{-1} \sim 2\,\mathrm{GeV}$, again determined from charmonium 1S-1P splitting in two-flavour QCD. Using 1-loop perturbation theory with boosted coupling, they obtain $\alpha_V^{(2)} = 0.169$ and $\alpha_{\overline{\mathrm{MS}}}^{(2)} = 0.142$. Davies 94 [133] gives a determination of α_V from the expansion

$$-\ln W_{11} \equiv \frac{4\pi}{3} \alpha_V^{(N_f)}(3.41/a) \times [1 - (1.185 + 0.070 N_f)\alpha_V^{(N_f)}], \qquad (324)$$

neglecting higher-order terms. They compute the Υ spectrum in $N_f = 0,\ 2$ QCD for single lattice spacings at $a^{-1} = 2.57,\ 2.47\,\mathrm{GeV}$ and obtain $\alpha_V(3.41/a) \simeq 0.15,\ 0.18$, respectively. Extrapolating the inverse coupling linearly in N_f, a value of $\alpha_V^{(3)}(8.3\,\mathrm{GeV}) = 0.196(3)$ is obtained. SESAM 99 [131] follows a similar strategy, again for a single lattice spacing. They linearly extrapolated results for $1/\alpha_V^{(0)}$, $1/\alpha_V^{(2)}$ at a fixed scale of $9\,\mathrm{GeV}$ to give $\alpha_V^{(3)}$, which is then perturbatively converted to $\alpha_{\overline{\mathrm{MS}}}^{(3)}$. This finally gave $\alpha_{\overline{\mathrm{MS}}}^{(5)}(M_Z) = 0.1118(17)$. Wingate 95 [132] also follows this method. With the scale determined from the charmonium 1S-1P

Collaboration	Ref.	N_f	publication status	renormalization scale	perturbative behaviour	lattice spacings	scale	$\Lambda_{\overline{\mathrm{MS}}}$[MeV]	$r_0\Lambda_{\overline{\mathrm{MS}}}$
HPQCD 10$^{a\,\S}$	[128]	2+1	A	○	★	★	$r_1 = 0.3133(23)$ fm	340(9)	0.812(22)
HPQCD 08A^a	[125]	2+1	A	○	★	★	$r_1 = 0.321(5)$ fm††	338(12)*	0.809(29)
Maltman 08^a	[129]	2+1	A	○	○	★	$r_1 = 0.318$ fm	352(17)†	0.841(40)
HPQCD 05A^a	[124]	2+1	A	○	○	○	$r_1^{\dagger\dagger}$	319(17)**	0.763(42)
QCDSF/UKQCD 05	[130]	2	A	★	■	★	$r_0 = 0.467(33)$ fm	261(17)(26)	0.617(40)(21)^b
SESAM 99^c	[131]	2	A	○	■	■	$c\bar{c}$(1S-1P)		
Wingate 95^d	[132]	2	A	★	■	■	$c\bar{c}$(1S-1P)		
Davies 94^e	[133]	2	A	★	■	■	Υ		
Aoki 94^f	[134]	2	A	★	■	■	$c\bar{c}$(1S-1P)		
Kitazawa 16	[35]	0	A	★	★	★	w_0	260(5)^j	0.621(11)^j
FlowQCD 15	[26]	0	P	★	★	★	$w_{0.4}{}^i$	258(6)^i	0.618(11)^i
QCDSF/UKQCD 05	[130]	0	A	★	○	★	$r_0 = 0.467(33)$ fm	259(1)(20)	0.614(2)(5)^b
SESAM 99^c	[131]	0	A	★	■	■	$c\bar{c}$(1S-1P)		
Wingate 95^d	[132]	0	A	★	■	■	$c\bar{c}$(1S-1P)		
Davies 94^e	[133]	0	A	★	■	■	Υ		
El-Khadra 92^g	[135]	0	A	★	■	○	$c\bar{c}$(1S-1P)	234(10)	0.560(24)^h

^{a} The numbers for Λ have been converted from the values for $\alpha_s^{(5)}(M_Z)$.

§ $\alpha_{\overline{\mathrm{MS}}}^{(3)}(5\text{ GeV}) = 0.2034(21)$, $\alpha_{\overline{\mathrm{MS}}}^{(5)}(M_Z) = 0.1184(6)$, only update of intermediate scale and c-, b-quark masses, supersedes HPQCD 08A.

† $\alpha_{\overline{\mathrm{MS}}}^{(5)}(M_Z) = 0.1192(11)$.

* $\alpha_V^{(3)}(7.5\text{ GeV}) = 0.2120(28)$, $\alpha_{\overline{\mathrm{MS}}}^{(5)}(M_Z) = 0.1183(8)$, supersedes HPQCD 05.

†† Scale is originally determined from Υ mass splitting. r_1 is used as an intermediate scale. In conversion to $r_0\Lambda_{\overline{\mathrm{MS}}}$, r_0 is taken to be 0.472 fm.

** $\alpha_V^{(3)}(7.5\text{ GeV}) = 0.2082(40)$, $\alpha_{\overline{\mathrm{MS}}}^{(5)}(M_Z) = 0.1170(12)$.

^{b} This supersedes Refs. [136–138]. $\alpha_{\overline{\mathrm{MS}}}^{(5)}(M_Z) = 0.112(1)(2)$. The $N_f = 2$ results were based on values for r_0/a which have later been found to be too small [57]. The effect will be of the order of 10–15%, presumably an increase in Λr_0.

^{c} $\alpha_{\overline{\mathrm{MS}}}^{(5)}(M_Z) = 0.1118(17)$.

^{d} $\alpha_V^{(3)}(6.48\text{ GeV}) = 0.194(7)$ extrapolated from $N_f = 0, 2$. $\alpha_{\overline{\mathrm{MS}}}^{(5)}(M_Z) = 0.107(5)$.

^{e} $\alpha_P^{(3)}(8.2\text{ GeV}) = 0.1959(34)$ extrapolated from $N_f = 0, 2$. $\alpha_{\overline{\mathrm{MS}}}^{(5)}(M_Z) = 0.115(2)$.

^{f} Estimated $\alpha_{\overline{\mathrm{MS}}}^{(5)}(M_Z) = 0.108(5)(4)$.

^{g} This early computation violates our requirement that scheme conversions are done at the 2-loop level. $\Lambda_{\overline{\mathrm{MS}}}^{(4)} = 160(^{+47}_{-37})$MeV, $\alpha_{\overline{\mathrm{MS}}}^{(4)}(5\text{GeV}) = 0.174(12)$. We converted this number to give $\alpha_{\overline{\mathrm{MS}}}^{(5)}(M_Z) = 0.106(4)$.

^{h} We used $r_0 = 0.472$ fm to convert to $r_0\Lambda_{\overline{\mathrm{MS}}}$.

^{i} Reference scale $w_{0.4}$ where w_x is defined by $t\partial_t[t^2\langle E(t)\rangle]\big|_{t=w_x^2} = x$ in terms of the action density $E(t)$ at positive flow time t [26]. Our conversion to r_0 scale using [26] $r_0/w_{0.4} = 2.587(45)$ and $r_0 = 0.472$ fm.

^{j} Our conversion from $w_0\Lambda_{\overline{\mathrm{MS}}} = 0.2154(12)$ to r_0 scale using $r_0/w_0 = (r_0/w_{0.4}) \cdot (w_{0.4}/w_0) = 2.885(50)$ with the factors cited by the collaboration [26] and with $r_0 = 0.472$ fm.

Table 56: Wilson loop results. Some early results for $N_f = 0, 2$ did not determine $\Lambda_{\overline{\mathrm{MS}}}$.

splitting for single lattice spacings in $N_f = 0$, 2 giving $a^{-1} \simeq 1.80\,\text{GeV}$ for $N_f = 0$ and $a^{-1} \simeq 1.66\,\text{GeV}$ for $N_f = 2$, they obtain $\alpha_V^{(0)}(3.41/a) \simeq 0.15$ and $\alpha_V^{(2)} \simeq 0.18$, respectively. Extrapolating the coupling linearly in N_f, they obtain $\alpha_V^{(3)}(6.48\,\text{GeV}) = 0.194(17)$.

The QCDSF/UKQCD collaboration, QCDSF/UKQCD 05 [130], [136–138], use the 2-loop relation (re-written here in terms of α)

$$\frac{1}{\alpha_{\overline{\text{MS}}}(\mu)} = \frac{1}{\alpha_{\text{P}}(1/a)} + 4\pi(2b_0 \ln a\mu - t_1^{\text{P}}) + (4\pi)^2(2b_1 \ln a\mu - t_2^{\text{P}})\alpha_{\text{P}}(1/a) \,, \tag{325}$$

where t_1^{P} and t_2^{P} are known. (A 2-loop relation corresponds to a 3-loop lattice β-function.) This was used to directly compute $\alpha_{\overline{\text{MS}}}$, and the scale was chosen so that the $\mathcal{O}(\alpha_{\text{P}}^0)$ term vanishes, i.e.,

$$\mu^* = \frac{1}{a} \exp\left[t_1^{\text{P}}/(2b_0)\right] \approx \left\{ \begin{array}{ll} 2.63/a & N_f = 0 \\ 1.4/a & N_f = 2 \end{array} \right. . \tag{326}$$

The method is to first compute $\alpha_{\text{P}}(1/a)$ and from this, using Eq. (323) to find $\alpha_{\overline{\text{MS}}}(\mu^*)$. The RG equation, Eq. (280), then determines $\mu^*/\Lambda_{\overline{\text{MS}}}$ and hence using Eq. (324) leads to the result for $r_0\Lambda_{\overline{\text{MS}}}$. This avoids giving the scale in MeV until the end. In the $N_f = 0$ case seven lattice spacings were used [62], giving a range $\mu^*/\Lambda_{\overline{\text{MS}}} \approx 24$–72 (or $a^{-1} \approx 2$–7 GeV) and $\alpha_{\text{eff}} = \alpha_{\overline{\text{MS}}}(\mu^*) \approx 0.15$–0.10. Neglecting higher-order perturbative terms (see discussion after Eq. (325) below) in Eq. (323) this is sufficient to allow a continuum extrapolation of $r_0\Lambda_{\overline{\text{MS}}}$. A similar computation for $N_f = 2$ by QCDSF/UKQCD 05 [130] gave $\mu^*/\Lambda_{\overline{\text{MS}}} \approx 12$–17 (or roughly $a^{-1} \approx 2$–3 GeV) and $\alpha_{\text{eff}} = \alpha_{\overline{\text{MS}}}(\mu^*) \approx 0.20$–0.18. The $N_f = 2$ results of QCDSF/UKQCD 05 [130] are affected by an uncertainty which was not known at the time of publication: It has been realized that the values of r_0/a of Ref. [130] were significantly too low [57]. As this effect is expected to depend on a, it influences the perturbative behaviour leading us to assign a ■ for that criterion.

Since FLAG 13, there has been one new result for $N_f = 0$ by FlowQCD 15 [26], later updated and published in Kitazawa 16 [35]. They also use the techniques as described in Eqs. (323), (324), but together with the gradient flow scale w_0 (rather than the r_0 scale) leading to a determination of $w_0\Lambda_{\overline{\text{MS}}}$. The continuum limit is estimated by extrapolating the data at 6 lattice spacings linearly in a^2. The data range used is $\mu^*/\Lambda_{\overline{\text{MS}}} \approx 50$–120 (or $a^{-1} \approx 5$–11 GeV) and $\alpha_{\overline{\text{MS}}}(\mu^*) \approx 0.12$–0.095. Since a very small value of $\alpha_{\overline{\text{MS}}}$ is reached, there is a ★ in the perturbative behaviour. Note that our conversion to the common r_0 scale unfortunately leads to a significant increase of the error of the Λ parameter compared to using w_0 directly [68]. Again we note that the results of QCDSF/UKQCD 05 [130] ($N_f = 0$) and Kitazawa 16 [35] may be affected by frozen topology as they have lattice spacings significantly below $a = 0.05\,\text{fm}$. Kitazawa 16 [35] investigate this by evaluating w_0/a in a fixed topology and estimate any effect at about $\sim 1\%$.

The work of HPQCD 05A [124] (which supersedes the original work [139]) uses three lattice spacings $a^{-1} \approx 1.2$, 1.6, 2.3 GeV for $2+1$ flavour QCD. Typically the renormalization scale $q \approx \pi/a \approx 3.50$–7.10 GeV, corresponding to $\alpha_{\text{V}'} \approx 0.22$–0.28.

In the later update HPQCD 08A [125] twelve data sets (with six lattice spacings) are now used reaching up to $a^{-1} \approx 4.4\,\text{GeV}$, corresponding to $\alpha_{\text{V}'} \approx 0.18$. The values used for the scale r_1 were further updated in HPQCD 10 [128]. Maltman 08 [129] uses most of the same lattice ensembles as HPQCD 08A [125], but not the one at the smallest lattice spacing, $a \approx 0.045\,\text{fm}$. Maltman 08 [129] also considers a much smaller set of quantities (three versus

22) that are less sensitive to condensates. They also use different strategies for evaluating the condensates and for the perturbative expansion, and a slightly different value for the scale r_1. The central values of the final results from Maltman 08 [129] and HPQCD 08A [125] differ by 0.0009 (which would be decreased to 0.0007 taking into account a reduction of 0.0002 in the value of the r_1 scale used by Maltman 08 [129]).

As mentioned before, the perturbative coefficients are computed through 3-loop order [140], while the higher-order perturbative coefficients c_n with $n_{\max} \geq n > 3$ (with $n_{\max} = 10$) are numerically fitted using the lattice-simulation data for the lattice spacings with the help of Bayesian methods. It turns out that corrections in Eq. (319) are of order $|c_i/c_1|\alpha^i = 5\text{–}15\%$ and 3–10% for $i = 2, 3$, respectively. The inclusion of a fourth-order term is necessary to obtain a good fit to the data, and leads to a shift of the result by $1 - 2$ sigma. For all but one of the 22 quantities, central values of $|c_4/c_1| \approx 2\text{–}4$ were found, with errors from the fits of ≈ 2.

An important source of uncertainty is the truncation of perturbation theory. In HPQCD 08A [125], 10 [128] it is estimated to be about 0.4% of $\alpha_{\overline{\text{MS}}}(M_Z)$. In FLAG 13 we included a rather detailed discussion of the issue with the result that we prefer for the time being a more conservative error based on the above estimate $|c_4/c_1| = 2$. From Eq. (318) this gives an estimate of the uncertainty in α_{eff} of

$$\Delta\alpha_{\text{eff}}(\mu_1) = \left|\frac{c_4}{c_1}\right|\alpha_{\text{eff}}^4(\mu_1)\,, \tag{327}$$

at the scale μ_1 where α_{eff} is computed from the Wilson loops. This can be used with a variation in Λ at lowest order of perturbation theory and also applied to α_s evolved to a different scale μ_2,[6]

$$\frac{\Delta\Lambda}{\Lambda} = \frac{1}{8\pi b_0\alpha_s}\frac{\Delta\alpha_s}{\alpha_s}\,, \qquad \frac{\Delta\alpha_s(\mu_2)}{\Delta\alpha_s(\mu_1)} = \frac{\alpha_s^2(\mu_2)}{\alpha_s^2(\mu_1)}\,. \tag{328}$$

With $\mu_2 = M_Z$ and $\alpha_s(\mu_1) = 0.2$ (a typical value extracted from Wilson loops in HPQCD 10 [128], HPQCD 08A [125] at $\mu = 5\,\text{GeV}$) we have

$$\Delta\alpha_{\overline{\text{MS}}}(m_Z) = 0.0012\,, \tag{329}$$

which we shall later use as the typical perturbative uncertainty of the method with $2 + 1$ fermions.

Tab. 56 summarizes the results. Within the errors of 3–5% $N_f = 3$ determinations of $r_0\Lambda$ nicely agree.

9.7 α_s from heavy-quark current two-point functions

9.7.1   General considerations

The method has been introduced in HPQCD 08, Ref. [141], and updated in HPQCD 10, Ref. [128], see also Ref. [142]. In addition there is a 2+1+1 flavour result, HPQCD 14A [27]. Since FLAG 16 two new results have appeared: JLQCD 16 [36] and Maezawa 16 [37].

---

[6]From Eq. (287) we see that at low order in PT the coupling α_s is continuous and differentiable across the mass thresholds (at the same scale). Therefore to leading order α_s and $\Delta\alpha_s$ are independent of N_f.

The basic observable is constructed from a current

$$J(x) = im_c \overline{\psi}_c(x) \gamma_5 \psi_{c'}(x) \tag{330}$$

of two mass-degenerate heavy-valence quarks, c, c', usually taken to be at or around the charm quark mass. The pre-factor m_c denotes the bare mass of the quark. When the lattice discretization respects chiral symmetry, $J(x)$ is a renormalization group invariant local field, i.e., it requires no renormalization. Staggered fermions and twisted mass fermions have such a residual chiral symmetry. The (Euclidean) time-slice correlation function

$$G(x_0) = a^3 \sum_{\vec{x}} \langle J^\dagger(x) J(0) \rangle \,, \tag{331}$$

$(J^\dagger(x) = im_c \overline{\psi}_{c'}(x) \gamma_5 \psi_c(x))$ has a $\sim x_0^{-3}$ singularity at short distances and moments

$$G_n = a \sum_{x_0 = -(T/2-a)}^{T/2-a} x_0^n \, G(x_0) \tag{332}$$

are nonvanishing for even n and furthermore finite for $n \geq 4$. Here T is the time extent of the lattice. The moments are dominated by contributions at t of order $1/m_c$. For large mass m_c these are short distances and the moments become increasingly perturbative for decreasing n. Denoting the lowest-order perturbation theory moments by $G_n^{(0)}$, one defines the normalized moments

$$R_n = \begin{cases} G_4/G_4^{(0)} & \text{for } n = 4 \,, \\ \frac{am_{\eta_c}}{2am_c} \left(\frac{G_n}{G_n^{(0)}} \right)^{1/(n-4)} & \text{for } n \geq 6 \,, \end{cases} \tag{333}$$

of even order n. Note that Eq. (328) contains the variable (bare) heavy-quark mass m_c. The normalization $G_n^{(0)}$ is introduced to help in reducing lattice artifacts. In addition, one can also define moments with different normalizations,

$$\tilde{R}_n = 2R_n/m_{\eta_c} \qquad \text{for } n \geq 6 \,. \tag{334}$$

While $\tilde{R}_n$ also remains renormalization group invariant, it now also has a scale which might introduce an additional ambiguity [36].

The normalized moments can then be parameterized in terms of functions

$$R_n \equiv \begin{cases} r_4(\alpha_s(\mu)) & \text{for } n = 4 \,, \\ \frac{r_n(\alpha_s(\mu))}{\bar{m}_c(\mu)} & \text{for } n \geq 6 \,, \end{cases} \tag{335}$$

with $\bar{m}_c(\mu)$ being the renormalized charm-quark mass. The reduced moments r_n have a perturbative expansion

$$r_n = 1 + r_{n,1}\alpha_s + r_{n,2}\alpha_s^2 + r_{n,3}\alpha_s^3 + \dots \,, \tag{336}$$

where the written terms $r_{n,i}(\mu/\bar{m}_c(\mu))$, $i \leq 3$ are known for low n from Refs. [143–147]. In practice, the expansion is performed in the $\overline{\text{MS}}$ scheme. Matching nonperturbative lattice results for the moments to the perturbative expansion, one determines an approximation

to $\alpha_{\overline{\mathrm{MS}}}(\mu)$ as well as $\bar{m}_c(\mu)$. With the lattice spacing (scale) determined from some extra physical input, this calibrates μ. As usual suitable pseudoscalar masses determine the bare quark masses, here in particular the charm mass, and then through Eq. (333) the renormalized charm-quark mass.

A difficulty with this approach is that large masses are needed to enter the perturbative domain. Lattice artifacts can then be sizeable and have a complicated form. The ratios in Eq. (331) use the tree-level lattice results in the usual way for normalization. This results in unity as the leading term in Eq. (334), suppressing some of the kinematical lattice artifacts. We note that in contrast to, e.g., the definition of α_{qq}, here the cutoff effects are of order $a^k \alpha_s$, while there the tree-level term defines α_s and therefore the cutoff effects after tree-level improvement are of order $a^k \alpha_s^2$.

Finite-size effects (FSE) due to the omission of $|t| > T/2$ in Eq. (330) grow with n as $(m_{\eta_c}T/2)^n \exp(-m_{\eta_c}T/2)$. In practice, however, since the (lower) moments are short-distance dominated, the FSE are expected to be irrelevant at the present level of precision.

Moments of correlation functions of the quark's electromagnetic current can also be obtained from experimental data for e^+e^- annihilation [148, 149]. This enables a nonlattice determination of α_s using a similar analysis method. In particular, the same continuum perturbation theory computation enters both the lattice and the phenomenological determinations.

9.7.2 Discussion of computations

The method has originally been applied in HPQCD 08B [141] and in HPQCD 10 [128], based on the MILC ensembles with $2+1$ flavours of Asqtad staggered quarks and HISQ valence quarks. Both use R_n while the latter also used a range of quark masses m_c in addition to the physical charm mass.

The scale was set using $r_1 = 0.321(5)\,\mathrm{fm}$ in HPQCD 08B [141] and the updated value $r_1 = 0.3133(23)\,\mathrm{fm}$ in HPQCD 10 [128]. The effective range of couplings used is here given for $n = 4$, which is the moment most dominated by short (perturbative) distances and important in the determination of α_s. The range is similar for other ratios. With $r_{4,1} = 0.7427$ and $R_4 = 1.28$ determined in the continuum limit at the charm mass in Ref. [141], we have $\alpha_{\mathrm{eff}} = 0.38$ at the charm-quark mass, which is the mass value where HPQCD 08B [141] carries out the analysis. In HPQCD 10 [128] a set of masses is used, with $\tilde{R}_4 \in [1.09, 1.29]$, which corresponds to $\alpha_{\mathrm{eff}} \in [0.12, 0.40]$. The available data of HPQCD 10 [128] is reviewed in FLAG 13. For the continuum limit criterion, we choose the scale $\mu = 2\bar{m}_c \approx m_{\eta_c}/1.1$, where we have taken $\bar{m}_c$ in the $\overline{\mathrm{MS}}$ scheme at scale $\bar{m}_c$ and the numerical value 1.1 was determined in HPQCD 10B [151]. With these choices for μ, the continuum limit criterion is satisfied for three lattice spacings when $\alpha_{\mathrm{eff}} \leq 0.3$ and $n = 4$.

Larger-n moments are more influenced by nonperturbative effects. For the n values considered, adding a gluon condensate term only changed error bars slightly in HPQCD's analysis. We note that HPQCD in their papers perform a global fit to all data using a joint expansion in powers of α_s^n, $(\Lambda/(m_{\eta_c}/2))^j$ to parameterize the heavy-quark mass dependence, and $(am_{\eta_c}/2)^{2i}$ to parameterize the lattice-spacing dependence. To obtain a good fit, they must exclude data with $am_{\eta_c} > 1.95$ and include lattice-spacing terms a^{2i} with i greater than 10. Because these fits include many more fit parameters than data points, HPQCD uses their expectations for the sizes of coefficients as Bayesian priors. The fits include data with masses as large as $am_{\eta_c}/2 \sim 0.86$, so there is only minimal suppression of the many high-order con-

Collaboration	Ref.	N_f	publication status	renormalization scale	perturbative behaviour	continuum extrapolation	scale	$\Lambda_{\overline{\mathrm{MS}}}[\mathrm{MeV}]$	$r_0\Lambda_{\overline{\mathrm{MS}}}$
HPQCD 14A	[27]	2+1+1	A	○	★	○	$w_0 = 0.1715(9)\,\mathrm{fm}^a$	$294(11)^{bc}$	$0.703(26)$
Maezawa 16	[37]	2+1	A	○	■	○	$r_1 = 0.3106(18)\,\mathrm{fm}^d$	$309(10)^e$	$0.739(24)^e$
JLQCD 16	[36]	2+1	A	○	○	○	$\sqrt{t_0} = 0.1465(25)\,\mathrm{fm}$	$331(38)^f$	$0.792(89)^f$
HPQCD 10	[128]	2+1	A	○	★	○	$r_1 = 0.3133(23)\,\mathrm{fm}^\dagger$	$338(10)^\star$	$0.809(25)$
HPQCD 08B	[141]	2+1	A	■	■	■	$r_1 = 0.321(5)\,\mathrm{fm}^\dagger$	$325(18)^+$	$0.777(42)$

^{a} Scale determined in [150] using f_π.
^{b} $\alpha_{\overline{\mathrm{MS}}}^{(4)}(5\,\mathrm{GeV}) = 0.2128(25)$, $\alpha_{\overline{\mathrm{MS}}}^{(5)}(M_Z) = 0.11822(74)$.
^{c} We evaluated $\Lambda_{\overline{\mathrm{MS}}}^{(4)}$ from $\alpha_{\overline{\mathrm{MS}}}^{(4)}$. We also used $r_0 = 0.472\,\mathrm{fm}$.
^{d} Scale is determined from f_π .
^{e} $\alpha_{\overline{\mathrm{MS}}}^{(3)}(m_c = 1.267\,\mathrm{GeV}) = 0.3697(85)$, $\alpha_{\overline{\mathrm{MS}}}^{(5)}(M_Z) = 0.11622(84)$. Our conversion with $r_0 = 0.472\,\mathrm{fm}$.
^{f} We evaluated $\Lambda_{\overline{\mathrm{MS}}}^{(3)}$ from the given $\alpha_{\overline{\mathrm{MS}}}^{(4)}(3\,\mathrm{GeV}) = 0.2528(127)$. $\alpha_{\overline{\mathrm{MS}}}^{(5)}(M_Z) = 0.1177(26)$. We also used $r_0 = 0.472\,\mathrm{fm}$ to convert.
* $\alpha_{\overline{\mathrm{MS}}}^{(3)}(5\,\mathrm{GeV}) = 0.2034(21)$, $\alpha_{\overline{\mathrm{MS}}}^{(5)}(M_Z) = 0.1183(7)$.
† Scale is determined from Υ mass splitting.
$^+$ We evaluated $\Lambda_{\overline{\mathrm{MS}}}^{(3)}$ from the given $\alpha_{\overline{\mathrm{MS}}}^{(4)}(3\,\mathrm{GeV}) = 0.251(6)$. $\alpha_{\overline{\mathrm{MS}}}^{(5)}(M_Z) = 0.1174(12)$.

Table 57: Heavy-quark current two-point function results. Note that all analysis using $2+1$ flavour simulations perturbatively add a dynamical charm quark. Partially they then quote results in $N_f = 4$-flavour QCD, which we converted back to $N_f = 3$, corresponding to the nonperturbative sea quark content.

tributions for the heavier masses. It is not clear, however, how sensitive the final results are to the larger $am_{\eta_c}/2$ values in the data. The continuum limit of the fit is in agreement with a perturbative scale dependence (a 5-loop running $\alpha_{\overline{\mathrm{MS}}}$ with a fitted 5-loop coefficient in the β-function is used). Indeed, Fig. 2 of Ref. [128] suggests that HPQCD's fit describes the data well.

A more recent computation, HPQCD 14A [27] uses $\tilde{R}_n$ and is based on MILC's $2+1+1$ HISQ staggered ensembles. Compared to HPQCD 10 [128] valence- and sea-quarks now use the same discretization and the scale is set through the gradient flow scale w_0, determined to $w_0 = 0.1715(9)\,\mathrm{fm}$ in Ref. [152]. A number of data points satisfy our continuum limit criterion $a\mu < 1.5$, at two different lattice spacings. This does not by itself lead to a ○ but the next-larger lattice spacing does not miss the criterion by much . We therefore assign a ○ in that criterion.

Two new computations have appeared since the last FLAG report. Maezawa and Petreczky, [37] computed the two-point functions of the $c\bar{c}$ pseudoscalar operator and obtained R_4, R_6/R_8 and R_8/R_{10} based on the HotQCD collaboration HISQ staggered ensembles, [52]. The scale is set by measuring $r_1 = 0.3106(18)$ fm. Continuum limits are taken fitting the lattice spacing dependence with $a^2 + a^4$ form as the best fit. For R_4, they also employ other

forms for fit functions such as a^2, $\alpha_s^{\mathrm{boosted}}a^2 + a^4$, etc., the results agreeing within errors. Matching R_4 with the 3-loop formula Eq. (334) through order $\alpha_{\overline{\mathrm{MS}}}^3$ [143], where μ is fixed to m_c, they obtain $\alpha_{\overline{\mathrm{MS}}}^{(3)}(\mu = m_c) = 0.3697(54)(64)(15)$. The first error is statistical, the second is the uncertainty in the continuum extrapolation, and the third is the truncation error in the perturbative approximation of r_4. This last error is estimated by the "typical size" of the missing 4-loop contribution, which they assume to be $\alpha_{\overline{\mathrm{MS}}}^4(\mu)$ multiplied by 2 times the 3-loop coefficient $2 \times r_{4,3} \times \alpha_{\overline{\mathrm{MS}}}^4(\mu) = 0.2364 \times \alpha_{\overline{\mathrm{MS}}}^4(\mu)$. The result is converted to

$$\alpha_{\overline{\mathrm{MS}}}^{(5)}(M_Z) = 0.11622(84) \,. \tag{337}$$

Since $\alpha_{\mathrm{eff}}(2m_c)$ reaches 0.25, we assign ○ for the criterion of the renormalization scale. As $\Delta\Lambda/\Lambda \sim \alpha_{\mathrm{eff}}^2$, we assign ■ for the criterion of perturbative behaviour. The lattice cutoff ranges as $a^{-1} = 1.42$–4.89 GeV with $\mu = 2m_c \sim 2.6$ GeV so that we assign ○ for continuum extrapolation.

JLQCD 16 [36] also computed the two-point functions of the $c\bar{c}$ pseudoscalar operator and obtained R_6, R_8, R_{10} and their ratios based on 2+1 flavour QCD with Möbius domain-wall quark for three lattice cutoff $a^{-1} = 2.5$, 3.6, 4.5 GeV. The scale is set by $\sqrt{t_0} = 0.1465(21)(13)$ fm. The continuum limit is taken assuming linear dependence on a^2. They find a sizeable lattice-spacing dependence of R_4, which is therefore not used in their analysis, but for R_6, R_8, R_{10} the dependence is mild giving reasonable control over the continuum limit. They use the perturbative formulae for the vacuum polarization in the pseudoscalar channel Π_{PS} through order $\alpha_{\overline{\mathrm{MS}}}^3$ in the $\overline{\mathrm{MS}}$ scheme [145, 146] to obtain $\alpha_{\overline{\mathrm{MS}}}^{(4)}$. Combining the matching of lattice results with continuum perturbation theory for R_6, R_6/R_8 and R_{10}, they obtain $\alpha_{\overline{\mathrm{MS}}}^{(4)}(\mu = 3 \text{ GeV}) = 0.2528(127)$, where the error is dominated by the perturbative truncation error. To estimate the truncation error they study the dependence of the final result on the choice of the renormalization scales μ_α, μ_{m} which are used as renormalization scales for α and the quark mass. Independently [153] the two scales are varied in the range of 2 GeV to 4 GeV. The above result is converted to $\alpha_{\overline{\mathrm{MS}}}^{(5)}(M_Z)$ as

$$\alpha_{\overline{\mathrm{MS}}}^{(5)}(M_Z) = 0.1177(26) \,. \tag{338}$$

Since α_{eff} roughly reaches 0.25, they have ○ for the renormalization scale criterion. Since $\Delta\Lambda/\Lambda > \alpha_{\mathrm{eff}}^2$, we also assign ○ for the criterion of perturbative behaviour. The lattice cutoff ranges over $a^{-1} = 2.5$–4.5 GeV with $\mu = 3$ GeV so we also give them a ○ for continuum extrapolation.

There is a significant difference in the perturbative error estimate of JLQCD 16 [36] and Maezawa 16 [37], both of which use the moments at the charm mass. JLQCD 16 uses the scale dependence (see also Sec. 9.2.3) but Maezawa 16 looks at the perturbative coefficients at $\mu = m_*$, with $\bar{m}_c(m_*) = m_*$. While the Maezawa 16 result derives from R_4, JLQCD 16 did not use that moment and therefore did not show its renormalization-scale dependence. We provide it here and show $\alpha(m_*)$ extracted from R_4 expanded in $\alpha(\mu)$ for $\mu = s \, m_*$ (and evolved to $\mu = m_*$) in Fig. 35. Note that the perturbative error estimated by Maezawa 16 is a small contribution to the total error, while the scale dependence in Fig. 35 is significant between, e.g., $s = 1$ and $s = 4$. This is a confirmation of our ■ in the perturbative error criterion which is linked to the cited overall error as spelled out in Sec. 9.2.1.

Aside from the final results for $\alpha_s(m_Z)$ obtained by matching with perturbation theory, it is interesting to make a comparison of the short distance quantities in the continuum limit
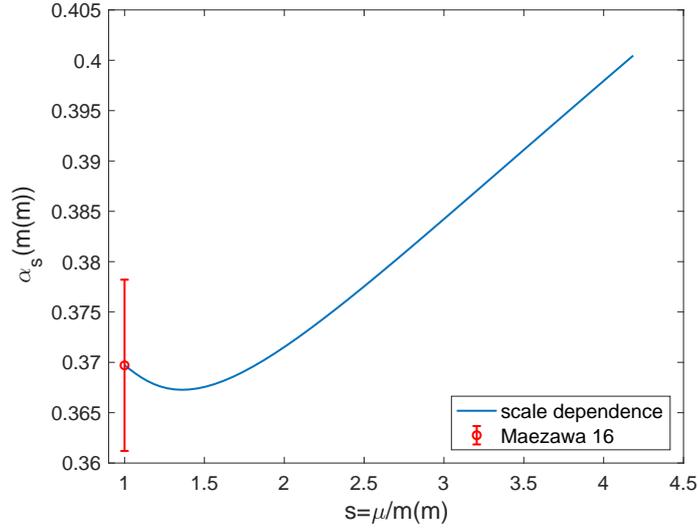
Figure 35: Renormalization-scale (μ) dependence of $\alpha(m_*)$ extracted from R_4. We have evaluated this dependence for the case where the same renormalization scale is used for the quark mass and for α_s.

R_n which are available from HPQCD 08 [141], JLQCD 16 [36] and Maezawa 16 [37] (all using $2 + 1$ flavours). In Fig 36 we plot the various results based on the numbers collated in
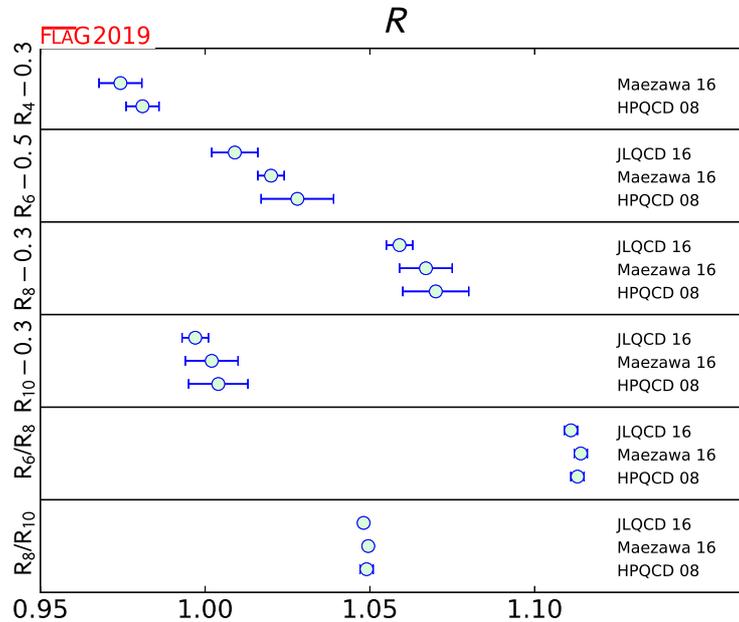

Figure 36: Ratios from Tab. 58. Note that constants have been subtracted from R_4, R_6 and R_{10}, to be able to plot all results in a similar range.

Tab. 58. These results are in quite good agreement with each other. For future studies it is of

	HPQCD 08	Maezawa 16	JLQCD 16
R_4	1.281(5)	1.274(7)	-
R_6	1.528(11)	1.520(4)	1.509(7)
R_8	1.370(10)	1.367(8)	1.359(4)
R_{10}	1.304(9)	1.302(8)	1.297(4)
R_6/R_8	1.113(2)	1.114(2)	1.111(2)
R_8/R_{10}	1.049(2)	1.0495(7)	1.0481(9)

Table 58: Moments from $N_f = 3$ simulations at the charm mass. The moments have been corrected perturbatively to include the effect of a charm sea quark.

course interesting to check agreement of these numbers before turning to the more involved determination of α_s.

In Tab. 57 we summarize the results for the latter.

9.8 α_s from QCD vertices

9.8.1   General considerations

The most intuitive and in principle direct way to determine the coupling constant in QCD is to compute the appropriate three- or four-point gluon vertices or alternatively the quark-quark-gluon vertex or ghost-ghost-gluon vertex (i.e., $q\bar{q}A$ or $c\bar{c}A$ vertex, respectively). A suitable combination of renormalization constants then leads to the relation between the bare (lattice) and renormalized coupling constant. This procedure requires the implementation of a nonperturbative renormalization condition and the fixing of the gauge. For the study of nonperturbative gauge fixing and the associated Gribov ambiguity, we refer to Refs. [154–156] and references therein. In practice the Landau gauge is used and the renormalization constants are defined by requiring that the vertex is equal to the tree level value at a certain momentum configuration. The resulting renormalization schemes are called 'MOM' scheme (symmetric momentum configuration) or '$\widetilde{\text{MOM}}$' (one momentum vanishes), which are then converted perturbatively to the $\overline{\text{MS}}$ scheme.

A pioneering work to determine the three-gluon vertex in the $N_f = 0$ theory is Alles 96 [157] (which was followed by Ref. [158] for two flavour QCD); a more recent $N_f = 0$ computation was Ref. [159] in which the three-gluon vertex as well as the ghost-ghost-gluon vertex was considered. (This requires a computation of the propagator of the Faddeev–Popov ghost on the lattice.) The latter paper concluded that the resulting $\Lambda_{\overline{\text{MS}}}$ depended strongly on the scheme used, the order of perturbation theory used in the matching and also on nonperturbative corrections [160].

Subsequently in Refs. [161, 162] a specific $\widetilde{\text{MOM}}$ scheme with zero ghost momentum for the ghost-ghost-gluon vertex was used. In this scheme, dubbed the 'MM' (Minimal MOM) or 'Taylor' (T) scheme, the vertex is not renormalized, and so the renormalized coupling reduces to

$$\alpha_{\text{T}}(\mu) = D_{\text{lat}}^{\text{gluon}}(\mu, a) D_{\text{lat}}^{\text{ghost}}(\mu, a)^2 \, \frac{g_0^2}{4\pi} \,, \tag{339}$$

where $D_{\text{lat}}^{\text{ghost}}$ and $D_{\text{lat}}^{\text{gluon}}$ are the (bare lattice) dressed ghost and gluon 'form factors' of these propagator functions in the Landau gauge,

$$D^{ab}(p) = -\delta^{ab} \frac{D^{\text{ghost}}(p)}{p^2} \,, \qquad D_{\mu\nu}^{ab}(p) = \delta^{ab} \left(\delta_{\mu\nu} - \frac{p_\mu p_\nu}{p^2} \right) \frac{D^{\text{gluon}}(p)}{p^2} \,, \qquad (340)$$

and we have written the formula in the continuum with $D^{\text{ghost/gluon}}(p) = D_{\text{lat}}^{\text{ghost/gluon}}(p, 0)$. Thus there is now no need to compute the ghost-ghost-gluon vertex, just the ghost and gluon propagators.

9.8.2 Discussion of computations

For the calculations considered here, to match to perturbative scaling, it was first necessary to reduce lattice artifacts by an $H(4)$ extrapolation procedure (addressing $O(4)$ rotational invariance), e.g., ETM 10F [168] or by lattice perturbation theory, e.g., Sternbeck 12 [166]. To match to perturbation theory, collaborations vary in their approach. In ETM 10F [168], it was necessary to include the operator A^2 in the OPE of the ghost and gluon propagators, while in Sternbeck 12 [166] very large momenta are used and $a^2 p^2$ and $a^4 p^4$ terms are included in their fit to the momentum dependence. A further later refinement was the introduction of higher nonperturbative OPE power corrections in ETM 11D [165] and ETM 12C [164]. Although the expected leading power correction, $1/p^4$, was tried, ETM finds good agreement with their data only when they fit with the next-to-leading-order term, $1/p^6$. The update ETM 13D [163] investigates this point in more detail, using better data with reduced statistical errors. They find that after again including the $1/p^6$ term they can describe their data over a large momentum range from about 1.75 GeV to 7 GeV.

In all calculations except for Sternbeck 10 [167], Sternbeck 12 [166] , the matching with the perturbative formula is performed including power corrections in the form of condensates, in particular $\langle A^2 \rangle$. Three lattice spacings are present in almost all calculations with $N_f = 0, 2$, but the scales ap are rather large. This mostly results in a ■ on the continuum extrapolation (Sternbeck 10 [167], Boucaud 01B [158] for $N_f = 2$. Ilgenfritz 10 [169], Boucaud 08 [162], Boucaud 05 [159], Becirevic 99B [174], Becirevic 99A [175], Boucaud 98B [176], Boucaud 98A [177], Alles 96 [157] for $N_f = 0$). A ○ is reached in the $N_f = 0$ computations Boucaud 00A [173], 00B [172], 01A [171], Soto 01 [170] due to a rather small lattice spacing, but this is done on a lattice of a small physical size. The $N_f = 2 + 1 + 1$ calculation, fitting with condensates, is carried out for two lattice spacings and with $ap > 1.5$, giving ■ for the continuum extrapolation as well. In ETM 10F [168] we have $0.25 < \alpha_{\text{eff}} < 0.4$, while in ETM 11D [165], ETM 12C [164] (and ETM 13 [178]) we find $0.24 < \alpha_{\text{eff}} < 0.38$, which gives a green circle in these cases for the renormalization scale. In ETM 10F [168] the values of ap violate our criterion for a continuum limit only slightly, and we give a ○ .

In Sternbeck 10 [167], the coupling ranges over $0.07 \le \alpha_{\text{eff}} \le 0.32$ for $N_f = 0$ and $0.19 \le \alpha_{\text{eff}} \le 0.38$ for $N_f = 2$ giving ★ and ○ for the renormalization scale, respectively. The fit with the perturbative formula is carried out without condensates, giving a satisfactory description of the data. In Boucaud 01A [171], depending on a, a large range of α_{eff} is used which goes down to 0.2 giving a ○ for the renormalization scale and perturbative behaviour, and several lattice spacings are used leading to ○ in the continuum extrapolation. The $N_f = 2$ computation Boucaud 01B [171], fails the continuum limit criterion because both $a\mu$ is too large and an unimproved Wilson fermion action is used. Finally in the conference proceedings Sternbeck 12 [166], the $N_f = 0, 2, 3$ coupling α_{T} is studied. Subtracting 1-loop lattice artifacts

Collaboration Ref.		N_f	publication status	renormalization scale	perturbative behaviour	continuum extrapolation	scale	$\Lambda_{\overline{MS}}$[MeV]	$r_0\Lambda_{\overline{MS}}$
ETM 13D	[163]	2+1+1	A	○	○	■	f_π	$314(7)(14)(10)^a$	$0.752(18)(34)(81)^\dagger$
ETM 12C	[164]	2+1+1	A	○	○	■	f_π	$324(17)^\S$	$0.775(41)^\dagger$
ETM 11D	[165]	2+1+1	A	○	○	■	f_π	$316(13)(8)(^{+0}_{-9})^\star$	$0.756(31)(19)(^{+0}_{-22})^\dagger$
Sternbeck 12	[166]	2+1	C				only running of α_s in Fig. 4		
Sternbeck 12	[166]	2	C				Agreement with $r_0\Lambda_{\overline{MS}}$ value of [57]		
Sternbeck 10	[167]	2	C	○	★	■		$251(15)^\#$	$0.60(3)(2)$
ETM 10F	[168]	2	A	○	○	○	f_π	$330(23)(22)(^{+0}_{-33})$	$0.72(5)^+$
Boucaud 01B	[158]	2	A	○	○	■	$K^* - K$	$264(27)^{\star\star}$	$0.669(69)$
Sternbeck 12	[166]	0	C				Agreement with $r_0\Lambda_{\overline{MS}}$ value of [112]		
Sternbeck 10	[167]	0	C	★	★	■		$259(4)^\#$	$0.62(1)$
Ilgenfritz 10	[169]	0	A	★	★	■	only running of α_s in Fig. 13		
Boucaud 08	[162]	0	A	○	★	■	$\sqrt{\sigma} = 445$ MeV	$224(3)(^{+8}_{-5})$	$0.59(1)(^{+2}_{-1})$
Boucaud 05	[159]	0	A	■	★	■	$\sqrt{\sigma} = 445$ MeV	$320(32)$	$0.85(9)$
Soto 01	[170]	0	A	○	○	○	$\sqrt{\sigma} = 445$ MeV	$260(18)$	$0.69(5)$
Boucaud 01A	[171]	0	A	○	○	○	$\sqrt{\sigma} = 445$ MeV	$233(28)$ MeV	$0.62(7)$
Boucaud 00B	[172]	0	A	○	○	○		only running of α_s	
Boucaud 00A	[173]	0	A	○	○	○	$\sqrt{\sigma} = 445$ MeV	$237(3)(^{+0}_{-10})$	$0.63(1)(^{+0}_{-3})$
Becirevic 99B	[174]	0	A	○	○	■	$\sqrt{\sigma} = 445$ MeV	$319(14)(^{+10}_{-20})$	$0.84(4)(^{+3}_{-5})$
Becirevic 99A	[175]	0	A	○	○	■	$\sqrt{\sigma} = 445$ MeV	$\lesssim 353(2)(^{+25}_{-15})$	$\lesssim 0.93(^{+7}_{-4})$
Boucaud 98B	[176]	0	A	■	○	■	$\sqrt{\sigma} = 445$ MeV	$295(5)(15)$	$0.78(4)$
Boucaud 98A	[177]	0	A	■	○	■	$\sqrt{\sigma} = 445$ MeV	$300(5)$	$0.79(1)$
Alles 96	[157]	0	A	■	■	■	$\sqrt{\sigma} = 440$ MeV^{++}	$340(50)$	$0.91(13)$

^{a} $\alpha_{\overline{MS}}^{(5)}(M_Z) = 0.1196(4)(8)(6)$.
† We use the 2+1 value $r_0 = 0.472$ fm.
§ $\alpha_{\overline{MS}}^{(5)}(M_Z) = 0.1200(14)$.
* First error is statistical; second is due to the lattice spacing and third is due to the chiral extrapolation. $\alpha_{\overline{MS}}^{(5)}(M_Z) = 0.1198(9)(5)(^{+0}_{-5})$.
$^\#$ In the paper only $r_0\Lambda_{\overline{MS}}$ is given, we converted to MeV with $r_0 = 0.472$ fm.
$^+$ The determination of r_0 from the f_π scale is found in Ref. [55].
** $\alpha_{\overline{MS}}^{(5)}(M_Z) = 0.113(3)(4)$.
$^{++}$ The scale is taken from the string tension computation of Ref. [113].

Table 59: Results for the gluon–ghost vertex.

and subsequently fitting with a^2p^2 and a^4p^4 additional lattice artifacts, agreement with the perturbative running is found for large momenta $(r_0^2p^2 > 600)$ without the need for power corrections. In these comparisons, the values of $r_0\Lambda_{\overline{MS}}$ from other collaborations are used. As no numbers are given, we have not introduced ratings for this study.

In Tab. 59 we summarize the results. Presently there are no $N_f \geq 3$ calculations of α_s from QCD vertices that satisfy the FLAG criteria to be included in the range.

9.9 α_s from the eigenvalue spectrum of the Dirac operator

9.9.1   General considerations

Consider the spectral density of the continuum Dirac operator

$$\rho(\lambda) = \frac{1}{V} \left\langle \sum_k (\delta(\lambda - i\lambda_k) + \delta(\lambda + i\lambda_k)) \right\rangle , \tag{341}$$

where V is the volume and λ_k are the eigenvalues of the Dirac operator in a gauge background.

Its perturbative expansion

$$\rho(\lambda) = \frac{3}{4\pi^2} \lambda^3 (1 - \rho_1 \bar{g}^2 - \rho_2 \bar{g}^4 - \rho_3 \bar{g}^6 + \mathrm{O}(\bar{g}^8)) , \tag{342}$$

is known including ρ_3 in the $\overline{\mathrm{MS}}$ scheme [179, 180]. In renormalization group improved form one sets the renormalization scale μ to $\mu = s\lambda$ with $s = \mathrm{O}(1)$ and the ρ_i are pure numbers. Nakayama 18 [38] initiated a study of $\rho(\lambda)$ in the perturbative regime. They prefer to consider μ independent from λ. Then ρ_i are polynomials in $\log(\lambda/\mu)$ of degree i. One may consider

$$F(\lambda) \equiv \frac{\partial \log(\rho(\lambda))}{\partial \log(\lambda)} = 3 - F_1 \bar{g}^2 - F_2 \bar{g}^4 - F_3 \bar{g}^6 - F_4 \bar{g}^8 + \mathrm{O}(\bar{g}^{10}) , \tag{343}$$

where the four coefficients F_i, again polynomials of degree i in $\log(\lambda/\mu)$, are known. Choosing instead the renormalization group improved form with $\mu = s\lambda$ in Eq. (340) would have led to

$$F(\lambda) = 3 - \bar{F}_2 \bar{g}^4(\lambda) - \bar{F}_3 \bar{g}^6(\lambda) - \bar{F}_4 \bar{g}^8(\lambda) + \mathrm{O}(\bar{g}^{10}) , \tag{344}$$

with pure numbers $\bar{F}_i$ and $\bar{F}_1 = 0$. Determinations of α_s can be carried out by a computation and continuum extrapolation of $\rho(\lambda)$ and/or $F(\lambda)$ at large λ. Such computations are made possible by the techniques of [38, 46, 181].

We note that according to our general discussions in terms of an effective coupling, we have $n_l = 2$; the 3-loop β function of a coupling defined from Eq. (340) or Eq. (342) is known. [7]

9.9.2   Discussion of computations

There is one pioneering result to date using this method by Nakayama 18 [38]. They computed the eigenmode distributions of the Hermitian operator $a^2 D_{\mathrm{ov}}^{\dagger}(m_f = 0, am_{\mathrm{PV}}) D_{\mathrm{ov}}(m_f = 0, am_{\mathrm{PV}})$ where D_{ov} is the overlap operator and m_{PV} is the Pauli–Villars regulator on ensembles with 2+1 flavours using Möbius domain-wall quarks for three lattice cutoff $a^{-1} = 2.5, 3.6, 4.5$ GeV, where $am_{\mathrm{PV}} = 3$ or ∞. The bare eigenvalues are converted to the $\overline{\mathrm{MS}}$ scheme at $\mu = 2\,\mathrm{GeV}$ by multiplying with the renormalization constant $Z_m(2\,\mathrm{GeV})$, which is then transformed to those renormalized at $\mu = 6\,\mathrm{GeV}$ using the renormalization group equation. The scale is set by $\sqrt{t_0} = 0.1465(21)(13)\,\mathrm{fm}$. The continuum limit is taken assuming a linear dependence in a^2, while the volume size is kept about constant: 2.6–2.8 fm.

---

[7]In the present situation, the effective coupling would be defined by $\bar{g}_{\lambda}^2(\mu) = \bar{F}_2^{-1/2}(3 - F(\lambda))^{1/2}$ with $\mu = \lambda$, preferably taken as the renormalization group invariant eigenvalue.

Choosing the renormalization scale $\mu = 6 \, \text{GeV}$, Nakayama 18 [38], extracted $\alpha_{\overline{\text{MS}}}^{(3)}(6 \, \text{GeV}) = 0.204(10)$. The result is converted to

$$\alpha_{\overline{\text{MS}}}^{(5)}(M_Z) = 0.1226(36) \,. \tag{345}$$

The lattice cutoff ranges over $a^{-1} = 2.5 - 4.5 \, \text{GeV}$ with $\mu = \lambda = 0.8 - 1.25 \, \text{GeV}$ yielding quite small values $a\mu$. However, our continuum limit criterion does not apply as it requires us to consider $\alpha_s = 0.3$. We thus deviate from the general rule and give a ○ which would result at the smallest value $\alpha_{\overline{\text{MS}}}(\mu) = 0.4$ considered by Nakayama 18 [38]. The values of $\alpha_{\overline{\text{MS}}}$ lead to a ■ for the renormalization scale, while perturbative behavior is rated ○.

In Tab. 60 we list this result.

Collaboration	Ref.	N_f	publication status	renormalization scale	perturbative behaviour	continuum extrapolation	scale	$\Lambda_{\overline{\text{MS}}}[\text{MeV}]$	$r_0\Lambda_{\overline{\text{MS}}}$
Nakayama 18	[38]	2+1	A	■	○	○	$\sqrt{t_0}$	409(60)*	0.978(144)

* $\alpha_{\overline{\text{MS}}}^{(5)}(M_Z) = 0.1226(36)$. $\Lambda_{\overline{\text{MS}}}$ determined by us using $\alpha_{\overline{\text{MS}}}^{(3)}(6 \, \text{GeV}) = 0.204(10)$. Uses $r_0 = 0.472 \, \text{fm}$

Table 60: Dirac eigenvalue result.

9.10 Summary

After reviewing the individual computations, we are now in a position to discuss the overall result. We first present the current status and for that briefly consider $r_0\Lambda$ with its flavour dependence from $N_f = 0$ to 4 flavours. Then we discuss the central $\alpha_{\overline{\text{MS}}}(M_Z)$ results, which just use $N_f \geq 3$, give ranges for each sub-group discussed previously, and give final FLAG average as well as an overall average together with the current PDG nonlattice numbers. Finally we return to $r_0\Lambda$, presenting our estimates for the various N_f.

9.10.1 The present situation

We first summarize the status of lattice-QCD calculations of the QCD scale $\Lambda_{\overline{\text{MS}}}$. Fig. 37 shows all the results for $r_0\Lambda_{\overline{\text{MS}}}$ discussed in the previous sections.

Many of the numbers are the ones given directly in the papers. However, when only $\Lambda_{\overline{\text{MS}}}$ in physical units (MeV) is available, we have converted them by multiplying with the value of r_0 in physical units. The notation used is full green squares for results used in our final average, while a lightly shaded green square indicates that there are no red squares in the previous colour coding but the computation does not enter the ranges because either it has been superseded by an update or it is not published. Red open squares mean that there is at least one red square in the colour coding.
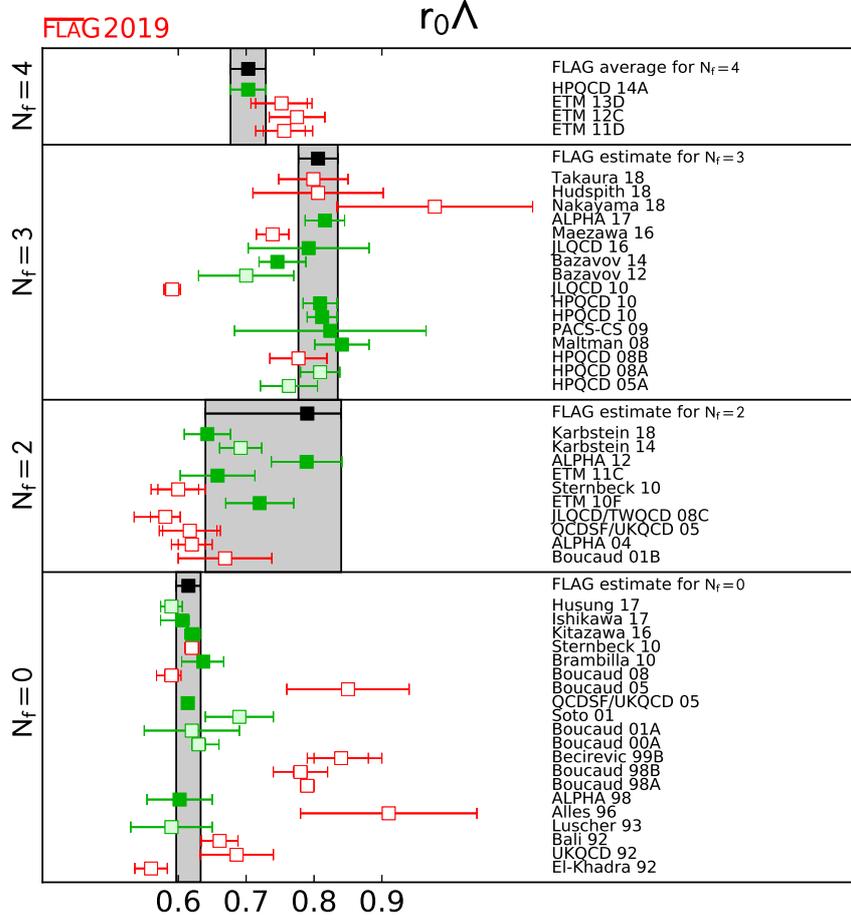
Figure 37: $r_0\Lambda_{\overline{MS}}$ estimates for $N_f = 0, 2, 3, 4$ flavours. Full green squares are used in our final ranges, pale green squares also indicate that there are no red squares in the colour coding but the computations were superseded by later more complete ones or not published, while red open squares mean that there is at least one red square in the colour coding.

For $N_f = 0$ there is relatively little spread in the more recent numbers.

When two flavours of quarks are included, the numbers extracted by the various groups show a considerable spread, as in particular older computations did not yet control the systematics sufficiently. This illustrates the difficulty of the problem and emphasizes the need for strict criteria. The agreement among the more modern calculations with three or more flavours, however, is quite good.

We now turn to the status of the essential result for phenomenology, $\alpha_{\overline{MS}}^{(5)}(M_Z)$. In Tab. 61 and the upper plot in Fig. 38 we show all the results for $\alpha_{\overline{MS}}^{(5)}(M_Z)$ (i.e., $\alpha_{\overline{MS}}$ at the Z mass) obtained from $N_f = 2 + 1$ and $N_f = 2 + 1 + 1$ simulations. The conversion from $N_f = 3$ or $N_f = 4$ to $N_f = 5$ is made by matching the coupling constant at the charm and bottom quark thresholds and using the scale as determined or used by the authors.

As can be seen from the tables and figures, at present there are several computations satisfying the criteria to be included in the FLAG average. Since FLAG 16 two new computations of $\alpha_{\overline{MS}}^{(5)}(M_Z)$ pass all our criteria with at least a ○ and one computation with all ★. The

Collaboration	Ref.	N_f	publication status	renormalization scale	perturbative behaviour	continuum extrapolation	$\alpha_{\overline{\text{MS}}}(M_Z)$	Remark	Tab.
ALPHA 17	[28]	2+1	A	★	★	★	0.11852(84)	step-scaling	53
PACS-CS 09A	[90]	2+1	A	★	★	○	0.11800(300)	step-scaling	53
pre-range (average)							0.11848(81)		
Takaura 18	[32, 33]	2+1	P	■	○	○	$0.11790(70)(^{+130}_{-120})$	Q-$\bar{Q}$ potential	54
Bazavov 14	[25]	2+1	A	○	★	○	0.11660(100)	Q-$\bar{Q}$ potential	54
Bazavov 12	[110]	2+1	A	○	○	○	$0.11560(^{+210}_{-220})$	Q-$\bar{Q}$ potential	54
pre-range with estimated pert. error							0.11660(160)		
Hudspith 18	[34]	2+1	P	○	★	■	$0.11810(270)(^{+80}_{-220})$	vacuum polarization	55
JLQCD 10	[120]	2+1	A	■	○	■	$0.11180(30)(^{+160}_{-170})$	vacuum polarization	55
HPQCD 10	[128]	2+1	A	○	★	★	0.11840(60)	Wilson loops	56
Maltman 08	[129]	2+1	A	○	○	★	0.11920(110)	Wilson loops	56
pre-range with estimated pert. error							0.11871(128)		
JLQCD 16	[36]	2+1	A	○	○	○	0.11770(260)	current two points	57
Maezawa 16	[37]	2+1	A	○	■	○	0.11622(84)	current two points	57
HPQCD 14A	[27]	2+1+1	A	○	★	○	0.11822(74)	current two points	57
HPQCD 10	[128]	2+1	A	○	★	○	0.11830(70)	current two points	57
HPQCD 08B	[141]	2+1	A	■	■	■	0.11740(120)	current two points	57
pre-range with estimated pert. error							0.11818(156)		
ETM 13D	[163]	2+1+1	A	○	○	■	0.11960(40)(80)(60)	gluon-ghost vertex	59
ETM 12C	[164]	2+1+1	A	○	○	■	0.12000(140)	gluon-ghost vertex	59
ETM 11D	[165]	2+1+1	A	○	○	■	$0.11980(90)(50)(^{+0}_{-50})$	gluon-ghost vertex	59
Nakayama 18	[38]	2+1	A	★	○	■	0.12260(360)	Dirac eigenvalues	60

Table 61: Results for $\alpha_{\overline{\text{MS}}}(M_Z)$. Different methods are listed separately and they are combined to a pre-range when computations are available without any ■ . A weighted average of the pre-ranges gives 0.11824(58), using the smallest pre-range uncertainty gives 0.11824(81) while the average uncertainty of the ranges used as an error gives 0.11824(131). We note that Bazavov 12 is superseded by Bazavov 14.

results agree quite well within the stated uncertainties. The uncertainties vary significantly.
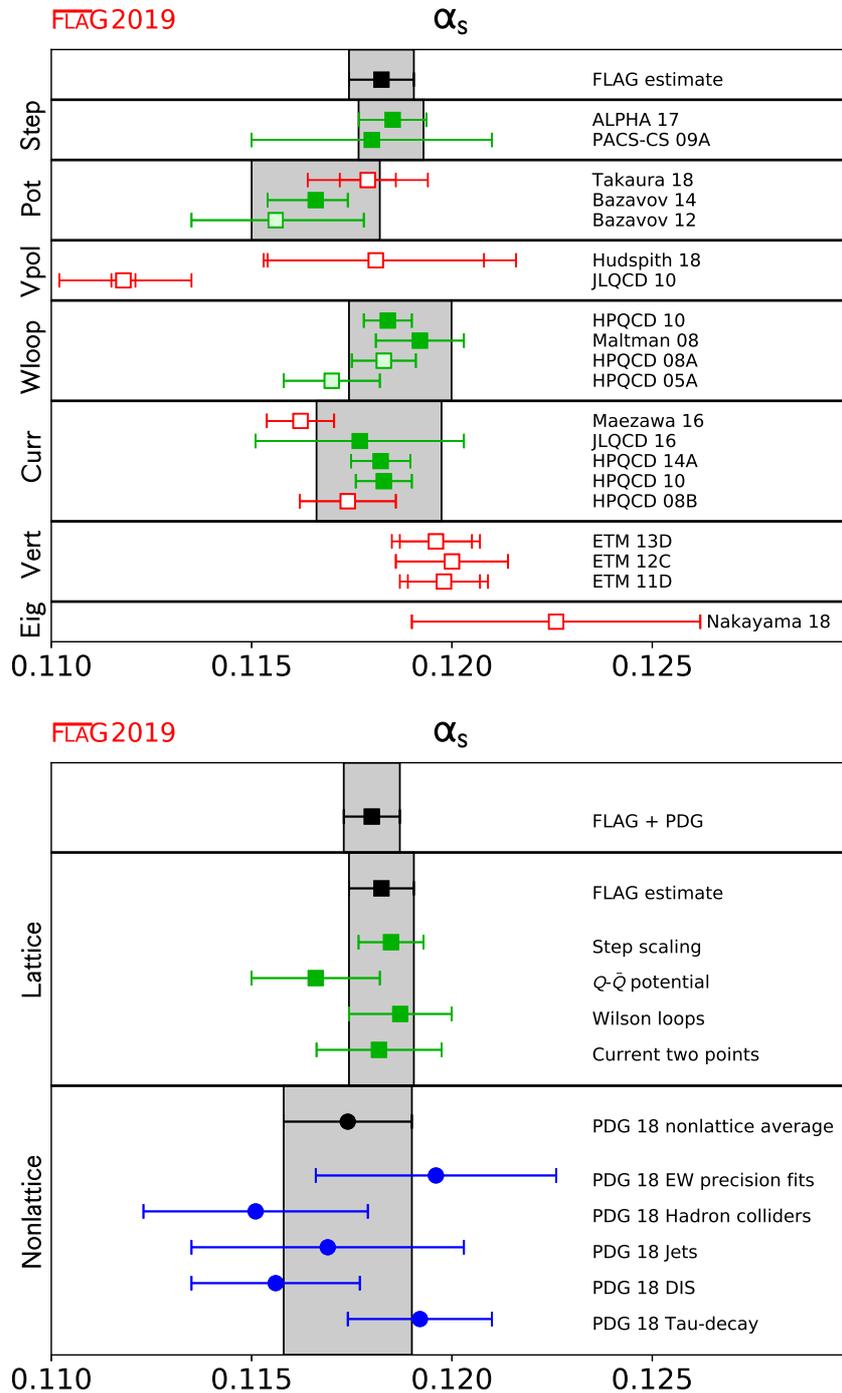
Figure 38: $\alpha^{(5)}_{\overline{\mathrm{MS}}}(M_Z)$, the coupling constant in the $\overline{\mathrm{MS}}$ scheme at the Z mass. Top: lattice results, pre-ranges from different calculation methods, and final average. Bottom: comparison of the lattice pre-ranges and average with the nonlattice ranges and average. The first PDG 18 entry gives the outcome of their analysis excluding lattice results (see Sec. 9.10.4).

9.10.2   Our range for $\alpha_{\overline{\mathrm{MS}}}^{(5)}$

We now explain the determination of our range. We only include those results without a red tag and that are published in a refereed journal. We also do not include any numbers that were obtained by extrapolating from theories with less than three flavours. They are not controlled and can be looked up in the previous FLAG reviews.

A general issue with most determinations of $\alpha_{\overline{\mathrm{MS}}}$, both lattice and nonlattice, is that they are dominated by perturbative truncation errors, which are difficult to estimate. Further, all results discussed here except for those of Secs. 9.3, 9.6 are based on extractions of $\alpha_{\overline{\mathrm{MS}}}$ that are largely influenced by data with $\alpha_{\mathrm{eff}} \geq 0.3$. At smaller α_s the momentum scale μ quickly is at or above a^{-1}. We have included computations using $a\mu$ up to 1.5 and α_{eff} up to 0.4, but one would ideally like to be significantly below that. Accordingly we choose to not simply perform weighted averages with the individual errors estimated by each group. Rather, we use our own more conservative estimates of the perturbative truncation errors in the weighted average.

In the following we repeat aspects of the methods and calculations that inform our estimates of the perturbative truncation errors. We also provide separate estimates for α_s obtained from step-scaling, the heavy-quark potential, Wilson loops, and heavy-quark current two-point functions to enable a comparison of the different lattice approaches; these are summarized in Tab. 61.

- *Step-scaling*
  The step-scaling computations of PACS-CS 09A [90] and ALPHA 17 [28] reach energies around the Z-mass where perturbative uncertainties in the three-flavour theory are negligible. Perturbative errors do enter in the conversion of the Λ-parameters from three to five flavours, but successive order contributions decrease rapidly and can be neglected. We form a weighted average of the two results and obtain $\alpha_{\overline{\mathrm{MS}}} = 0.11848(81)$.

- *Potential computations*
  Brambilla 10 [112], ETM 11C [111] and Bazavov 12 [110] give evidence that they have reached distances where perturbation theory can be used. However, in addition to Λ, a scale is introduced into the perturbative prediction by the process of subtracting the renormalon contribution. This subtraction is avoided in Bazavov 14 [25] by using the force and again agreement with perturbative running is reported. Husung 17 [30] (unpublished) studies the reliability of perturbation theory in the pure gauge theory with lattice spacings down to $0.015\,\mathrm{fm}$ and finds that at weak coupling there is a downwards trend in the Λ-parameter with a slope $\Delta\Lambda/\Lambda \approx 9\alpha_s^3$. While it is not very satisfactory to use just Husung 17 [30] to estimate the perturbative error, we do not have additional information at present. Further studies are needed to better understand the errors of α_s determinations from the potential.

  Only Bazavov 14 [25] satisfies all of the criteria to enter the FLAG average for α_s. Given the findings of [30] we estimate a perturbative error of $\Delta\Lambda/\Lambda = 9(\alpha_s^{\mathrm{min}})^3$ with $\alpha_s^{\mathrm{min}} \approx 0.19$ the smallest value reached in [25]. This translates into $\Delta\alpha_{\overline{\mathrm{MS}}}(M_Z) = 0.0014$. A different way to estimate the effect is to take the actual difference of the Λ-parameters estimated in $N_f = 0$ by Brambilla 10 [112] and Husung 17 [30]: $\Delta\Lambda/\Lambda \approx (0.637 - 0.590)/0.637 = 0.074$ or $\Delta\alpha_{\overline{\mathrm{MS}}}(M_Z) = 0.0018$. We use the mean of these two error estimates together with the central value of Bazavov 14 and obtain $\alpha_{\overline{\mathrm{MS}}} = 0.1166(16)$.

- *Small Wilson loops*
  Here the situation is unchanged as compared to FLAG 16. In the determination of α_s from observables at the lattice spacing scale, there is an interplay of higher-order perturbative terms and lattice artifacts. In HPQCD 05A [124], HPQCD 08A [125] and Maltman 08 [129] both lattice artifacts (which are power corrections in this approach) and higher-order perturbative terms are fitted. We note that Maltman 08 [129] and HPQCD 08A [125] analyze largely the same data set but use different versions of the perturbative expansion and treatments of nonperturbative terms. After adjusting for the slightly different lattice scales used, the values of $\alpha_{\overline{\mathrm{MS}}}(M_Z)$ differ by 0.0004 to 0.0008 for the three quantities considered. In fact the largest of these differences (0.0008) comes from a tadpole-improved loop, which is expected to be best behaved perturbatively. We therefore replace the perturbative-truncation errors from [129] and [128] with our estimate of the perturbative uncertainty Eq. (327). Taking the perturbative errors to be 100% correlated between the results, we obtain for the weighted average $\alpha_{\overline{\mathrm{MS}}} = 0.11871(128)$.

- *Heavy quark current two-point functions*
  Other computations with small errors are HPQCD 10 [128] and HPQCD 14A [27], where correlation functions of heavy valence quarks are used to construct short-distance quantities. Due to the large quark masses needed to reach the region of small coupling, considerable discretization errors are present, see Fig. 30 of FLAG 16. These are treated by fits to the perturbative running (a 5-loop running $\alpha_{\overline{\mathrm{MS}}}$ with a fitted 5-loop coefficient in the β-function is used) with high-order terms in a double expansion in $a^2\Lambda^2$ and $a^2 m_{\mathrm{c}}^2$ supplemented by priors which limit the size of the coefficients. The priors play an especially important role in these fits given the much larger number of fit parameters than data points. We note, however, that the size of the coefficients does not prevent high-order terms from contributing significantly, since the data includes values of am_{c} that are rather close to 1.

  More recent calculations use the same method but just at the charm quark mass, where discretization errors are considerably smaller. Here the dominating uncertainty is the perturbative error. JLQCD 16 [36] estimates it at $\Delta\alpha_s = 0.0011$ from independent changes of the renormalization scales of coupling and mass, $\mu_\alpha, \mu_{\mathrm{m}}$. Fig. 35 for the residual scale dependence of α_s from R_4 yields 0.0017 from scale change $1 \leq s \leq 3$ and 0.0025 for $2 \leq s \leq 4$. For the figure we set $\mu_\alpha = \mu_{\mathrm{m}}$. Independent changes of $\mu_\alpha, \mu_{\mathrm{m}}$ would yield a larger estimate of the uncertainty [153]. We note also that there are small differences in the continuum-extrapolated results in the moments themselves, cf. Tab. 58. The relative difference in $R_6/R_8 - 1 \sim k\alpha_s$ between Maezawa 16 [37], and JLQCD 16 [36], is about 4.5(2.5)%, which translates into a difference of 0.0023(13) in α_s at the Z-mass, close to the total cited uncertainty of JLQCD 16 [36]. A further estimate of the uncertainty is the difference of the JLQCD 16 [36] and Maezawa 16 [37] final numbers,[8] which is $\Delta\alpha_{\overline{\mathrm{MS}}}(M_Z) = 0.0015$

  We settle for an intermediate value of $\Delta\alpha_s = 0.0015$. Replacing the perturbative truncation errors from HPQCD 10 [128], HPQCD 14A [27], and JLQCD 16 [36] with this

---

[8]One may wonder why we consider Maezawa 16 which has a ■ in the perturbative behaviour. This rating is, however, due to the overall estimated uncertainty, not to the rest of the data and analysis, which we use here.

value, and including a 100% correlation between the perturbative errors, we obtain for the weighted average $\alpha_{\overline{\text{MS}}} = 0.11818(156)$.

- *Other methods*
  Computations using other methods do not qualify for an average yet, predominantly due to a lacking ○ in the continuum extrapolation.

We obtain the central value for our range of α_s from the weighted average of the four pre-ranges listed in Tab. 61. The error of this weighted average is 0.0006, which is quite a bit smaller than the most precise entry. Because, however, the errors on almost all of the α_s calculations that enter the average are dominated by perturbative truncation errors, which are especially difficult to estimate, we choose instead to take a larger range for α_s of 0.0008. This is the error on the pre-range for α_s from step-scaling, because perturbative-truncation errors are sub-dominant in this method. Our final range is then given by

$$\alpha_{\overline{\text{MS}}}^{(5)}(M_Z) = 0.1182(8) \,. \tag{346}$$

Almost all of the eight calculations that are included are within 1σ of this range. Further, the range for $\alpha_{\overline{\text{MS}}}^{(5)}(M_Z)$ presented here is based on results with rather different systematics (apart from the matching across the charm threshold). We therefore believe that the true value is very likely to lie within this range.

All computations which enter this range, with the exception of HPQCD 14A [27], rely on a perturbative inclusion of the charm and bottom quarks. Perturbation theory for the matching of $\bar{g}_{N_f}^2$ and $\bar{g}_{N_f-1}^2$ looks very well behaved even at the mass of the charm. Worries that still there may be purely nonperturbative effects at this rather low scale have been removed by nonperturbative studies of the accuracy of perturbation theory. While the original study in Ref. [183] was not precise enough, the extended one in Ref. [184] estimates effects in the Λ-parameter to be significantly below 1% and thus negligible for the present and near future accuracy.

9.10.3   Ranges for $[r_0\Lambda]^{(N_f)}$ and $\Lambda_{\overline{\text{MS}}}$

In the present situation, we give ranges for $[r_0\Lambda]^{(N_f)}$ and $\Lambda_{\overline{\text{MS}}}$, discussing their determination case by case. We include results with $N_f < 3$ because it is interesting to see the N_f-dependence of the connection of low- and high-energy QCD. This aids our understanding of the field theory and helps in finding possible ways to tackle it beyond the lattice approach. It is also of interest in providing an impression on the size of the vacuum polarization effects of quarks, in particular with an eye on the still difficult-to-treat heavier charm and bottom quarks. Even if this information is rather qualitative, it may be valuable, given that it is of a completely nonperturbative nature. We emphasize that results for $[r_0\Lambda]^{(0)}$ and $[r_0\Lambda]^{(2)}$ are *not* meant to be used in phenomenology.

For $N_f = 2 + 1 + 1$, we presently do not quote a range as there is a single result: HPQCD 14A [27] found $[r_0\Lambda]^{(4)} = 0.70(3)$.

For $N_f = 2+1$, we take as a central value the weighted average of ALPHA 17 [28], JLQCD 16 [36], Bazavov 14 [25], HPQCD 10 [128] (Wilson loops and current two-point correlators), PACS-CS 09A [90] and Maltman 08 [129]. Since the uncertainty in r_0 is small compared to that of Λ, we can directly propagate the error from the analog of Eq. (344) with the 2+1+1

number removed and arrive at

$$[r_0\Lambda_{\overline{\text{MS}}}]^{(3)} = 0.806(29) \, . \tag{347}$$

(The error of the straight weighted average is 0.012.) It is in good agreement with all 2+1 results without red tags. In physical units, using $r_0 = 0.472$ fm and neglecting its error, this means

$$\Lambda_{\overline{\text{MS}}}^{(3)} = 343(12) \, \text{MeV} \, , \tag{348}$$

where the error of the straight weighted average is 5 MeV.

For $N_f = 2$, at present there is one computation with a ★ rating for all criteria, ALPHA 12 [57]. We adopt it as our central value and enlarge the error to cover the central values of the other three results with filled green boxes. This results in an asymmetric error. Our range is unchanged as compared to FLAG 13,

$$[r_0\Lambda_{\overline{\text{MS}}}]^{(2)} = 0.79(^{+5}_{-15}) \, , \tag{349}$$

and in physical units, using $r_0 = 0.472$fm,

$$\Lambda_{\overline{\text{MS}}}^{(2)} = 330(^{+21}_{-63})\text{MeV} \, . \tag{350}$$

A weighted average of the four eligible numbers would yield $[r_0\Lambda_{\overline{\text{MS}}}]^{(2)} = 0.689(23)$, not covering the best result and in particular leading to a smaller error than we feel is justified, given the issues discussed previously in Sec. 9.4.2 (Karbstein 18 [31], ETM 11C [111]) and Sec. 9.8.2 (ETM 10F [168]). Thus we believe that our estimate is a conservative choice; the low values of ETM 11C [111] and Karbstein 18 [31] lead to a large downward error. We note that this can largely be explained by different values of r_0 between ETM 11C [111] and ALPHA 12 [57]. We still hope that future work will improve the situation.

For $N_f = 0$ we take into account ALPHA 98 [93], QCDSF/UKQCD 05 [130], Brambilla 10 [112], Kitazawa 16 [35] and Ishikawa 17 [29] for forming a range.[9] Taking a weighted average of the five numbers, we obtain $[r_0\Lambda_{\overline{\text{MS}}}]^{(0)} = 0.615(5)$, dominated by the QCDSF/UKQCD 05 [130] result.

Since the errors are dominantly systematic, due to missing higher orders of PT, we prefer to presently take a range which encompasses all five central values and whose uncertainty comes close to our estimate of the perturbative error in QCDSF/UKQCD 05 [130]: based on $|c_4/c_1| \approx 2$ as before, we find $\Delta[r_0\Lambda_{\overline{\text{MS}}}]^{(0)} = 0.018$. We then have

$$[r_0\Lambda_{\overline{\text{MS}}}]^{(0)} = 0.615(18) \, . \tag{351}$$

Converting to physical units, again using $r_0 = 0.472$ fm yields

$$\Lambda_{\overline{\text{MS}}}^{(0)} = 257(7) \, \text{MeV} \, . \tag{352}$$

While the conversion of the Λ parameter to physical units is quite unambiguous for $N_f = 2+1$, our choice of $r_0 = 0.472$ fm also for smaller numbers of flavour amounts to a convention, in

---

[9]We have assigned a ○ for the continuum limit, in Boucaud 00A [173], 00B [172], 01A [171], Soto 01 [170] but these results are from lattices of a very small physical size with finite-size effects that are not easily quantified.

particular for $N_f = 0$. Indeed, in the Tabs. 53–59 somewhat different numbers in MeV are found.

How sure are we about our ranges for $[r_0 \Lambda_{\overline{\text{MS}}}]^{(N_f)}$? In one case we have a result, Eq. (347) that easily passes our criteria; in another one [Eq. (349)] we have four compatible results that are close to that quality and agree. For $N_f = 2 + 1$ the range [Eq. (345)] takes account of results with rather different systematics. We therefore find it difficult to imagine that the ranges could be violated by much.

9.10.4   Conclusions

With the present results our range for the strong coupling is (repeating Eq. (344))

$$\alpha_{\overline{\text{MS}}}^{(5)}(M_Z) = 0.1182(8) \qquad \text{Refs. [25, 27, 28, 36, 90, 128, 129]},$$

and the associated Λ parameters

$$\Lambda_{\overline{\text{MS}}}^{(5)} = 211(10) \text{ MeV} \qquad \text{Refs. [25, 27, 28, 36, 90, 128, 129]}, \tag{353}$$

$$\Lambda_{\overline{\text{MS}}}^{(4)} = 294(12) \text{ MeV} \qquad \text{Refs. [25, 27, 28, 36, 90, 128, 129]}, \tag{354}$$

$$\Lambda_{\overline{\text{MS}}}^{(3)} = 343(12) \text{ MeV} \qquad \text{Refs. [25, 27, 28, 36, 90, 128, 129]}. \tag{355}$$

Compared with FLAG 16, the errors have been reduced by about 30% due to new computations. As can be seen from Fig. 38, when surveying the green data points, the individual lattice results agree within their quoted errors. Furthermore those points are based on different methods for determining α_s, each with its own difficulties and limitations. Thus the overall consistency of the lattice α_s results and the large number of ★ in Tab. 38, engenders confidence in our range.

It is interesting to compare with the Particle Data Group average of nonlattice determinations of recent years,

$$\alpha_{\overline{\text{MS}}}^{(5)}(M_Z) \quad = \quad 0.1174(16) \,, \quad \text{PDG 18, nonlattice [9]} \tag{279}$$

$$\alpha_{\overline{\text{MS}}}^{(5)}(M_Z) \quad = \quad 0.1174(16) \,, \quad \text{PDG 16, nonlattice [185]} \tag{356}$$

$$\alpha_{\overline{\text{MS}}}^{(5)}(M_Z) \quad = \quad 0.1175(17) \,, \quad \text{PDG 14, nonlattice [10]} \tag{357}$$

$$\alpha_{\overline{\text{MS}}}^{(5)}(M_Z) \quad = \quad 0.1183(12) \,, \quad \text{PDG 12, nonlattice [186]} \tag{358}$$

(there was no update in [9]). There is good agreement with Eq. (344). Due to recent new determinations the lattice average is by now a factor two more precise than the nonlattice world average and an average of the two [Eq. (344) and Eq. (279)] yields

$$\alpha_{\overline{\text{MS}}}^{(5)}(M_Z) \quad = \quad 0.1180(7) \,, \quad \text{FLAG 19 + PDG 18.} \tag{359}$$

In the lower plot in Fig. 38 we show as blue circles the various PDG pre-averages which lead to the PDG 2018/2016 nonlattice average. They are on a similar level as our pre-ranges (green squares) : each one corresponds to an estimate (by the PDG) of α_s determined from one set of input quantities. Within each pre-average multiple groups did the analysis and published

their results as displayed in Ref. [9]. The PDG performed an average within each group;[10] we only display the latter in Fig. 38.

The fact that our range for the lattice determination of $\alpha_{\overline{\text{MS}}}(M_Z)$ in Eq. (344) is in excellent agreement with the PDG nonlattice average Eq. (279) is an excellent check for the subtle interplay of theory, phenomenology and experiments in the nonlattice determinations. The work done on the lattice provides an entirely independent determination, with negligible experimental uncertainty, which reaches a better precision even with our quite conservative estimate of its uncertainty.

Given that the PDG has not updated their number, Eq. (357) is presently the up-to-date world average.

We finish by commenting on perspectives for the future. The step-scaling methods have been shown to yield a very precise result and to satisfy all criteria easily. A downside is that dedicated simulations have to be done and the method is thus hardly used. It would be desirable to have at least one more such computation by an independent collaboration, as also requested in the review [11]. For now, we have seen a decrease of the error by 30% compared to FLAG 16. There is potential for a further reduction. Likely there will be more lattice calculations of α_s from different quantities and by different collaborations. This will enable increasingly precise determinations, coupled with stringent cross-checks.

---

[10]Note that these are not straight weighted averages since often individual results within one group are not in good agreement.

References

[1] S. Dittmaier et al., *Handbook of LHC Higgs Cross Sections: 2. Differential Distributions*, 1201.3084.

[2] LHC Higgs Cross Section Working Group collaboration, S. Heinemeyer et al., *Handbook of LHC Higgs Cross Sections: 3. Higgs Properties*, 1307.1347.

[3] LBNE collaboration, C. Adams et al., *Scientific Opportunities with the Long-Baseline Neutrino Experiment*, 1307.7335.

[4] S. Dawson, A. Gritsan, H. Logan, J. Qian, C. Tully et al., *Higgs Working Group Report of the Snowmass 2013 Community Planning Study*, 1310.8361.

[5] A. Accardi et al., *A critical appraisal and evaluation of modern PDFs*, *Eur. Phys. J.* **C76** (2016) 471, [1603.08906].

[6] G. P. Lepage, P. B. Mackenzie and M. E. Peskin, *Expected Precision of Higgs Boson Partial Widths within the Standard Model*, 1404.0319.

[7] D. Buttazzo, G. Degrassi, P. P. Giardino, G. F. Giudice, F. Sala, A. Salvio et al., *Investigating the near-criticality of the Higgs boson*, *JHEP* **12** (2013) 089, [1307.3536].

[8] J. R. Espinosa, *Vacuum Stability and the Higgs Boson*, *PoS* **LATTICE2013** (2014) 010, [1311.1970].

[9] Particle Data Group collaboration, M. Tanabashi et al., *Review of Particle Physics*, *Phys. Rev.* **D98** (2018) 030001.

[10] Particle Data Group collaboration, K. A. Olive et al., *Review of Particle Physics*, *Chin. Phys.* **C38** (2014) 090001 and 2015 update.

[11] G. P. Salam, *The strong coupling: a theoretical perspective*, in *From My Vast Repertoire ...: Guido Altarelli's Legacy* (A. Levy, S. Forte and G. Ridolfi, eds.), pp. 101–121. 2019. 1712.05165. DOI.

[12] W. Bernreuther and W. Wetzel, *Decoupling of heavy quarks in the minimal subtraction scheme*, *Nucl.Phys.* **B197** (1982) 228.

[13] K. Chetyrkin, J. H. Kuhn and C. Sturm, *QCD decoupling at four loops*, *Nucl.Phys.* **B744** (2006) 121–135, [hep-ph/0512060].

[14] Y. Schröder and M. Steinhauser, *Four-loop decoupling relations for the strong coupling*, *JHEP* **01** (2006) 051, [hep-ph/0512058].

[15] B. A. Kniehl, A. V. Kotikov, A. I. Onishchenko and O. L. Veretin, *Strong-coupling constant with flavor thresholds at five loops in the anti-MS scheme*, *Phys. Rev. Lett.* **97** (2006) 042001, [hep-ph/0607202].

[16] T. van Ritbergen, J. A. M. Vermaseren and S. A. Larin, *The four-loop β-function in Quantum Chromodynamics*, *Phys. Lett.* **B400** (1997) 379–384, [hep-ph/9701390].

[17] M. Czakon, *The Four-loop QCD beta-function and anomalous dimensions*, *Nucl. Phys.* **B710** (2005) 485–498, [hep-ph/0411261].

[18] T. Luthe, A. Maier, P. Marquard and Y. Schröder, *Towards the five-loop Beta function for a general gauge group*, *JHEP* **07** (2016) 127, [1606.08662].

[19] F. Herzog, B. Ruijl, T. Ueda, J. A. M. Vermaseren and A. Vogt, *The five-loop beta function of Yang-Mills theory with fermions*, *JHEP* **02** (2017) 090, [1701.01404].

[20] P. A. Baikov, K. G. Chetyrkin and J. H. Kuhn, *Five-Loop Running of the QCD coupling constant*, *Phys. Rev. Lett.* **118** (2017) 082002, [1606.08659].

[21] A. G. Grozin, M. Hoeschele, J. Hoff and M. Steinhauser, *Simultaneous decoupling of bottom and charm quarks*, *JHEP* **09** (2011) 066, [1107.5970].

[22] K. G. Chetyrkin, J. H. Kuhn and M. Steinhauser, *RunDec: A Mathematica package for running and decoupling of the strong coupling and quark masses*, *Comput. Phys. Commun.* **133** (2000) 43–65, [hep-ph/0004189].

[23] F. Herren and M. Steinhauser, *Version 3 of RunDec and CRunDec*, *Comput. Phys. Commun.* **224** (2018) 333–345, [1703.03751].

[24] F. Karbstein, A. Peters and M. Wagner, $\Lambda_{\overline{\text{MS}}}^{(n_f=2)}$ *from a momentum space analysis of the quark-antiquark static potential*, *JHEP* **1409** (2014) 114, [1407.7503].

[25] A. Bazavov, N. Brambilla, X. Garcia i Tormo, P. Petreczky, S. J. and A. Vairo, *Determination of α_s from the QCD static energy: An update*, *Phys.Rev.* **D90** (2014) 074038, [1407.8437].

[26] [FlowQCD 15] M. Asakawa, T. Iritani, M. Kitazawa and H. Suzuki, *Determination of Reference Scales for Wilson Gauge Action from Yang–Mills Gradient Flow*, 1503.06516.

[27] [HPQCD 14A] B. Chakraborty, C. T. H. Davies, G. C. Donald, R. J. Dowdall, B. Galloway, P. Knecht et al., *High-precision quark masses and QCD coupling from $n_f = 4$ lattice QCD*, *Phys.Rev.* **D91** (2015) 054508, [1408.4169].

[28] [ALPHA 17] M. Bruno, M. Dalla Brida, P. Fritzsch, T. Korzec, A. Ramos, S. Schaefer et al., *QCD Coupling from a Nonperturbative Determination of the Three-Flavor Λ Parameter*, *Phys. Rev. Lett.* **119** (2017) 102001, [1706.03821].

[29] K.-I. Ishikawa, I. Kanamori, Y. Murakami, A. Nakamura, M. Okawa and R. Ueno, *Non-perturbative determination of the Λ-parameter in the pure SU(3) gauge theory from the twisted gradient flow coupling*, *JHEP* **12** (2017) 067, [1702.06289].

[30] N. Husung, M. Koren, P. Krah and R. Sommer, *SU(3) Yang Mills theory at small distances and fine lattices*, *EPJ Web Conf.* **175** (2018) 14024, [1711.01860].

[31] F. Karbstein, M. Wagner and M. Weber, *Determination of $\Lambda_{\overline{MS}}^{(n_f=2)}$ and analytic parameterization of the static quark-antiquark potentialDetermination of $\Lambda_{\overline{MS}}^{(n_f=2)}$ and analytic parametrization of the static quark-antiquark potential*, *Phys. Rev.* **D98** (2018) 114506, [1804.10909].

[32] H. Takaura, T. Kaneko, Y. Kiyo and Y. Sumino, *Determination of α_s from static QCD potential with renormalon subtraction*, *Phys. Lett.* **B789** (2019) 598–602, [1808.01632].

[33] H. Takaura, T. Kaneko, Y. Kiyo and Y. Sumino, *Determination of α_s from static QCD potential: OPE with renormalon subtraction and Lattice QCD*, *JHEP* **04** (2019) 155, [1808.01643].

[34] R. J. Hudspith, R. Lewis, K. Maltman and E. Shintani, *α_s from the Lattice Hadronic Vacuum Polarisation*, 1804.10286.

[35] M. Kitazawa, T. Iritani, M. Asakawa, T. Hatsuda and H. Suzuki, *Equation of State for SU(3) Gauge Theory via the Energy-Momentum Tensor under Gradient Flow*, *Phys. Rev.* **D94** (2016) 114512, [1610.07810].

[36] [JLQCD 16] K. Nakayama, B. Fahy and S. Hashimoto, *Short-distance charmonium correlator on the lattice with Möbius domain-wall fermion and a determination of charm quark mass*, *Phys. Rev.* **D94** (2016) 054507, [1606.01002].

[37] Y. Maezawa and P. Petreczky, *Quark masses and strong coupling constant in 2+1 flavor QCD*, *Phys. Rev.* **D94** (2016) 034507, [1606.08798].

[38] K. Nakayama, H. Fukaya and S. Hashimoto, *Lattice computation of the Dirac eigenvalue density in the perturbative regime of QCD*, *Phys. Rev.* **D98** (2018) 014501, [1804.06695].

[39] M. Lüscher, *Properties and uses of the Wilson flow in lattice QCD*, *JHEP* **08** (2010) 071, [1006.4518].

[40] [BMW 12A] S. Borsanyi, S. Dürr, Z. Fodor, C. Hoelbling, S. D. Katz et al., *High-precision scale setting in lattice QCD*, *JHEP* **1209** (2012) 010, [1203.4469].

[41] R. Sommer, *A new way to set the energy scale in lattice gauge theories and its applications to the static force and α_s in SU(2) Yang-Mills theory*, *Nucl. Phys.* **B411** (1994) 839–854, [hep-lat/9310022].

[42] C. W. Bernard et al., *The static quark potential in three flavor QCD*, *Phys. Rev.* **D62** (2000) 034503, [hep-lat/0002028].

[43] G. Martinelli and C. T. Sachrajda, *On the difficulty of computing higher twist corrections*, *Nucl.Phys.* **B478** (1996) 660–686, [hep-ph/9605336].

[44] S. Bethke, A. H. Hoang, S. Kluth, J. Schieck, I. W. Stewart et al., *Workshop on Precision Measurements of α_s*, 1110.0016.

[45] D. Boito, M. Golterman, K. Maltman, J. Osborne and S. Peris, *Strong coupling from the revised ALEPH data for hadronic τ decays*, *Phys. Rev.* **D91** (2015) 034003, [1410.3528].

[46] D. Boito, M. Golterman, K. Maltman and S. Peris, *Strong coupling from hadronic τ decays: A critical appraisal*, *Phys. Rev.* **D95** (2017) 034024, [1611.03457].

[47] L. Del Debbio, H. Panagopoulos and E. Vicari, *Theta dependence of SU(N) gauge theories*, *JHEP* **08** (2002) 044, [`hep-th/0204125`].

[48] C. Bernard et al., *Topological susceptibility with the improved Asqtad action*, *Phys. Rev.* **D68** (2003) 114501, [`hep-lat/0308019`].

[49] [ALPHA 10C] S. Schaefer, R. Sommer and F. Virotta, *Critical slowing down and error analysis in lattice QCD simulations*, *Nucl.Phys.* **B845** (2011) 93–119, [`1009.5228`].

[50] A. Chowdhury, A. Harindranath, J. Maiti and P. Majumdar, *Topological susceptibility in lattice Yang-Mills theory with open boundary condition*, *JHEP* **02** (2014) 045, [`1311.6599`].

[51] [LSD 14] R. C. Brower et al., *Maximum-Likelihood Approach to Topological Charge Fluctuations in Lattice Gauge Theory*, *Phys. Rev.* **D90** (2014) 014503, [`1403.2761`].

[52] [HotQCD 14] A. Bazavov et al., *Equation of state in (2+1)-flavor QCD*, *Phys.Rev.* **D90** (2014) 094503, [`1407.6387`].

[53] [JLQCD 15] H. Fukaya, S. Aoki, G. Cossu, S. Hashimoto, T. Kaneko and J. Noaki, η' *meson mass from topological charge density correlator in QCD*, *Phys. Rev.* **D92** (2015) 111501, [`1509.00944`].

[54] M. Lüscher and S. Schaefer, *Lattice QCD without topology barriers*, *JHEP* **1107** (2011) 036, [`1105.4749`].

[55] [ETM 09C] R. Baron et al., *Light meson physics from maximally twisted mass lattice QCD*, *JHEP* **08** (2010) 097, [`0911.5061`].

[56] [ETM 09] B. Blossier et al., *Pseudoscalar decay constants of kaon and D-mesons from $N_f = 2$ twisted mass lattice QCD*, *JHEP* **0907** (2009) 043, [`0904.0954`].

[57] [ALPHA 12] P. Fritzsch, F. Knechtli, B. Leder, M. Marinkovic, S. Schaefer et al., *The strange quark mass and the Λ parameter of two flavor QCD*, *Nucl.Phys.* **B865** (2012) 397–429, [`1205.5380`].

[58] [QCDSF 12] G. Bali, P. Bruns, S. Collins, M. Deka, B. Glasle et al., *Nucleon mass and sigma term from lattice QCD with two light fermion flavors*, *Nucl.Phys.* **B866** (2013) 1–25, [`1206.7034`].

[59] [HPQCD 09B] C. T. H. Davies, E. Follana, I. Kendall, G. P. Lepage and C. McNeile, *Precise determination of the lattice spacing in full lattice QCD*, *Phys.Rev.* **D81** (2010) 034506, [`0910.1229`].

[60] [MILC 10] A. Bazavov et al., *Results for light pseudoscalar mesons*, *PoS* **LAT2010** (2010) 074, [`1012.0868`].

[61] [HotQCD 11] A. Bazavov, T. Bhattacharya, M. Cheng, C. DeTar, H. Ding et al., *The chiral and deconfinement aspects of the QCD transition*, *Phys.Rev.* **D85** (2012) 054503, [`1111.1710`].

[62] S. Necco and R. Sommer, *The $N_f = 0$ heavy quark potential from short to intermediate distances*, *Nucl.Phys.* **B622** (2002) 328–346, [`hep-lat/0108008`].

[63] M. Lüscher and P. Weisz, *Quark confinement and the bosonic string*, *JHEP* **0207** (2002) 049, [hep-lat/0207003].

[64] S. Sint and A. Ramos, *On O(a²) effects in gradient flow observables*, *PoS* **LATTICE2014** (2015) 329, [1411.6706].

[65] Z. Fodor, K. Holland, J. Kuti, S. Mondal, D. Nogradi et al., *The lattice gradient flow at tree-level and its improvement*, *JHEP* **1409** (2014) 018, [1406.0827].

[66] [MILC 15] A. Bazavov et al., *Gradient flow and scale setting on MILC HISQ ensembles*, *Phys. Rev.* **D93** (2016) 094510, [1503.02769].

[67] V. G. Bornyakov et al., *Wilson flow and scale setting from lattice QCD*, 1508.05916.

[68] R. Sommer, *Scale setting in lattice QCD*, *PoS* **LATTICE2013** (2014) 015, [1401.3270].

[69] [ALPHA 16] M. Dalla Brida, P. Fritzsch, T. Korzec, A. Ramos, S. Sint and R. Sommer, *Determination of the QCD Λ-parameter and the accuracy of perturbation theory at high energies*, *Phys. Rev. Lett.* **117** (2016) 182001, [1604.06193].

[70] [ALPHA 18] M. Dalla Brida, P. Fritzsch, T. Korzec, A. Ramos, S. Sint and R. Sommer, *A non-perturbative exploration of the high energy regime in $N_f = 3$ QCD*, *Eur. Phys. J.* **C78** (2018) 372, [1803.10230].

[71] M. Lüscher, P. Weisz and U. Wolff, *A numerical method to compute the running coupling in asymptotically free theories*, *Nucl.Phys.* **B359** (1991) 221–243.

[72] M. Lüscher, R. Narayanan, P. Weisz and U. Wolff, *The Schrödinger functional: a renormalizable probe for non-abelian gauge theories*, *Nucl. Phys.* **B384** (1992) 168–228, [hep-lat/9207009].

[73] S. Sint, *On the Schrödinger functional in QCD*, *Nucl.Phys.* **B421** (1994) 135–158, [hep-lat/9312079].

[74] A. Coste, A. Gonzalez-Arroyo, J. Jurkiewicz and C. Korthals Altes, *Zero momentum contribution to Wilson loops in periodic boxes*, *Nucl.Phys.* **B262** (1985) 67.

[75] M. Lüscher, R. Sommer, P. Weisz and U. Wolff, *A precise determination of the running coupling in the SU(3) Yang-Mills theory*, *Nucl.Phys.* **B413** (1994) 481–502, [hep-lat/9309005].

[76] S. Sint and R. Sommer, *The running coupling from the QCD Schrödinger functional: a one loop analysis*, *Nucl.Phys.* **B465** (1996) 71–98, [hep-lat/9508012].

[77] [ALPHA 99] A. Bode, P. Weisz and U. Wolff, *Two loop computation of the Schrödinger functional in lattice QCD*, *Nucl.Phys.* **B576** (2000) 517–539, [hep-lat/9911018].

[78] [CP-PACS 04] S. Takeda, S. Aoki, M. Fukugita, K.-I. Ishikawa, N. Ishizuka et al., *A scaling study of the step scaling function in SU(3) gauge theory with improved gauge actions*, *Phys.Rev.* **D70** (2004) 074510, [hep-lat/0408010].

[79] M. Lüscher, *A Semiclassical Formula for the Topological Susceptibility in a Finite Space-time Volume*, *Nucl. Phys.* **B205** (1982) 483.

[80] P. Fritzsch, A. Ramos and F. Stollenwerk, *Critical slowing down and the gradient flow coupling in the Schrdinger functional*, *PoS* **Lattice2013** (2014) 461, [1311.7304].

[81] M. Dalla Brida, P. Fritzsch, T. Korzec, A. Ramos, S. Sint and R. Sommer, *Slow running of the Gradient Flow coupling from 200 MeV to 4 GeV in $N_\mathrm{f} = 3$ QCD*, *Phys. Rev.* **D95** (2017) 014507, [1607.06423].

[82] M. Lüscher, *Step scaling and the Yang-Mills gradient flow*, *JHEP* **06** (2014) 105, [1404.5930].

[83] R. Narayanan and H. Neuberger, *Infinite N phase transitions in continuum Wilson loop operators*, *JHEP* **03** (2006) 064, [hep-th/0601210].

[84] Z. Fodor, K. Holland, J. Kuti, D. Nogradi and C. H. Wong, *The Yang-Mills gradient flow in finite volume*, *JHEP* **1211** (2012) 007, [1208.1051].

[85] P. Fritzsch and A. Ramos, *The gradient flow coupling in the Schrödinger functional*, *JHEP* **1310** (2013) 008, [1301.4388].

[86] A. Ramos, *The gradient flow running coupling with twisted boundary conditions*, *JHEP* **11** (2014) 101, [1409.1445].

[87] M. Dalla Brida and M. Lüscher, *SMD-based numerical stochastic perturbation theory*, *Eur. Phys. J.* **C77** (2017) 308, [1703.04396].

[88] [ALPHA 10A] F. Tekin, R. Sommer and U. Wolff, *The running coupling of QCD with four flavors*, *Nucl.Phys.* **B840** (2010) 114–128, [1006.0672].

[89] P. Perez-Rubio and S. Sint, *Non-perturbative running of the coupling from four flavour lattice QCD with staggered quarks*, *PoS* **LAT2010** (2010) 236, [1011.6580].

[90] [PACS-CS 09A] S. Aoki et al., *Precise determination of the strong coupling constant in $N_f = 2 + 1$ lattice QCD with the Schrödinger functional scheme*, *JHEP* **0910** (2009) 053, [0906.3906].

[91] [ALPHA 04] M. Della Morte et al., *Computation of the strong coupling in QCD with two dynamical flavours*, *Nucl. Phys.* **B713** (2005) 378–406, [hep-lat/0411025].

[92] [ALPHA 01A] A. Bode et al., *First results on the running coupling in QCD with two massless flavors*, *Phys.Lett.* **B515** (2001) 49–56, [hep-lat/0105003].

[93] [ALPHA 98] S. Capitani, M. Lüscher, R. Sommer and H. Wittig, *Nonperturbative quark mass renormalization in quenched lattice QCD*, *Nucl.Phys.* **B544** (1999) 669–698, [hep-lat/9810063].

[94] J. Bulava and S. Schaefer, *Improvement of $N_f = 3$ lattice QCD with Wilson fermions and tree-level improved gauge action*, *Nucl. Phys.* **B874** (2013) 188–197, [1304.7093].

[95] M. Lüscher and P. Weisz, *On-shell improved lattice gauge theories*, *Commun. Math. Phys.* **97** (1985) 59.

[96] [JLQCD/CP-PACS 04] N. Yamada et al., *Non-perturbative O(a)-improvement of Wilson quark action in three-flavor QCD with plaquette gauge action*, *Phys. Rev.* **D71** (2005) 054505, [`hep-lat/0406028`].

[97] [RBC/UKQCD 08] C. Allton et al., *Physical results from 2+1 flavor domain wall QCD and SU(2) chiral perturbation theory*, *Phys. Rev.* **D78** (2008) 114509, [`0804.0473`].

[98] A. Gonzalez-Arroyo and M. Okawa, *The string tension from smeared Wilson loops at large N*, *Phys. Lett.* **B718** (2013) 1524–1528, [`1206.0049`].

[99] C. Michael, *The running coupling from lattice gauge theory*, *Phys. Lett.* **B283** (1992) 103–106, [`hep-lat/9205010`].

[100] [UKQCD 92] S. P. Booth et al., *The running coupling from SU(3) lattice gauge theory*, *Phys. Lett.* **B294** (1992) 385–390, [`hep-lat/9209008`].

[101] W. Fischler, *Quark-antiquark potential in QCD*, *Nucl. Phys.* **B129** (1977) 157–174.

[102] A. Billoire, *How heavy must be quarks in order to build coulombic $q\bar{q}$ bound states*, *Phys. Lett.* **B92** (1980) 343.

[103] M. Peter, *The static potential in QCD: a full two loop calculation*, *Nucl. Phys.* **B501** (1997) 471–494, [`hep-ph/9702245`].

[104] Y. Schröder, *The static potential in QCD to two loops*, *Phys. Lett.* **B447** (1999) 321–326, [`hep-ph/9812205`].

[105] N. Brambilla, A. Pineda, J. Soto and A. Vairo, *The infrared behavior of the static potential in perturbative QCD*, *Phys. Rev.* **D60** (1999) 091502, [`hep-ph/9903355`].

[106] A. V. Smirnov, V. A. Smirnov and M. Steinhauser, *Three-loop static potential*, *Phys. Rev. Lett.* **104** (2010) 112002, [`0911.4742`].

[107] C. Anzai, Y. Kiyo and Y. Sumino, *Static QCD potential at three-loop order*, *Phys. Rev. Lett.* **104** (2010) 112003, [`0911.4335`].

[108] N. Brambilla, A. Vairo, X. Garcia i Tormo and J. Soto, *The QCD static energy at NNNLL*, *Phys. Rev.* **D80** (2009) 034016, [`0906.1390`].

[109] S. Necco and R. Sommer, *Testing perturbation theory on the $N_f = 0$ static quark potential*, *Phys. Lett.* **B523** (2001) 135–142, [`hep-ph/0109093`].

[110] A. Bazavov, N. Brambilla, X. Garcia i Tormo, P. Petreczky, J. Soto et al., *Determination of α_s from the QCD static energy*, *Phys. Rev.* **D86** (2012) 114031, [`1205.6155`].

[111] [ETM 11C] K. Jansen, F. Karbstein, A. Nagy and M. Wagner, $\Lambda_{\overline{MS}}$ *from the static potential for QCD with $N_f = 2$ dynamical quark flavors*, *JHEP* **1201** (2012) 025, [`1110.6859`].

[112] N. Brambilla, X. Garcia i Tormo, J. Soto and A. Vairo, *Precision determination of $r_0 \Lambda_{\overline{MS}}$ from the QCD static energy*, *Phys. Rev. Lett.* **105** (2010) 212001, [`1006.2066`].

[113] G. S. Bali and K. Schilling, *Running coupling and the Λ-parameter from SU(3) lattice simulations*, *Phys.Rev.* **D47** (1993) 661–672, [hep-lat/9208028].

[114] K. G. Chetyrkin, A. L. Kataev and F. V. Tkachov, *Higher Order Corrections to Sigma-t (e+ e- —¿ Hadrons) in Quantum Chromodynamics*, *Phys. Lett.* **85B** (1979) 277–279.

[115] L. R. Surguladze and M. A. Samuel, *Total hadronic cross-section in e+ e- annihilation at the four loop level of perturbative QCD*, *Phys. Rev. Lett.* **66** (1991) 560–563.

[116] S. G. Gorishnii, A. L. Kataev and S. A. Larin, *The $O(\alpha_s^3)$ corrections to $\sigma_{tot}(e^+e^- \to hadrons)$ and $\Gamma(\tau^- \to \nu_\tau + hadrons)$ in QCD*, *Phys. Lett.* **B259** (1991) 144–150.

[117] P. A. Baikov, K. G. Chetyrkin and J. H. Kuhn, *Order α_s^4 QCD Corrections to Z and tau Decays*, *Phys. Rev. Lett.* **101** (2008) 012002, [0801.1821].

[118] I. Balitsky, M. Beneke and V. M. Braun, *Instanton contributions to the τ decay widths*, *Phys.Lett.* **B318** (1993) 371–381, [hep-ph/9309217].

[119] R. J. Hudspith, R. Lewis, K. Maltman and E. Shintani, *Determining the QCD coupling from lattice vacuum polarization*, in *Proceedings, 33rd International Symposium on Lattice Field Theory (Lattice 2015)*, vol. LATTICE2015, p. 268, 2016. 1510.04890.

[120] [JLQCD 10] E. Shintani, S. Aoki, H. Fukaya, S. Hashimoto, T. Kaneko et al., *Strong coupling constant from vacuum polarization functions in three-flavor lattice QCD with dynamical overlap fermions*, *Phys.Rev.* **D82** (2010) 074505, Erratum–ibid. **D89** (2014) 099903, [1002.0371].

[121] [JLQCD/TWQCD 08C] E. Shintani et al., *Lattice study of the vacuum polarization function and determination of the strong coupling constant*, *Phys.Rev.* **D79** (2009) 074510, [0807.0556].

[122] [RBC/UKQCD 14B] T. Blum et al., *Domain wall QCD with physical quark masses*, *Phys. Rev.* **D93** (2016) 074505, [1411.7017].

[123] R. Hudspith, R. Lewis, K. Maltman and E. Shintani, *α_s from the Hadronic Vacuum Polarisation*, *EPJ Web Conf.* **175** (2018) 10006.

[124] [HPQCD 05A] Q. Mason et al., *Accurate determinations of α_s from realistic lattice QCD*, *Phys. Rev. Lett.* **95** (2005) 052002, [hep-lat/0503005].

[125] [HPQCD 08A] C. T. H. Davies et al., *Update: accurate determinations of α_s from realistic lattice QCD*, *Phys. Rev.* **D78** (2008) 114507, [0807.1687].

[126] G. P. Lepage and P. B. Mackenzie, *On the viability of lattice perturbation theory*, *Phys.Rev.* **D48** (1993) 2250–2264, [hep-lat/9209022].

[127] K. Hornbostel, G. Lepage and C. Morningstar, *Scale setting for α_s beyond leading order*, *Phys.Rev.* **D67** (2003) 034023, [hep-ph/0208224].

[128] [HPQCD 10] C. McNeile, C. T. H. Davies, E. Follana, K. Hornbostel and G. P. Lepage, *High-precision c and b masses and QCD coupling from current-current correlators in lattice and continuum QCD*, *Phys. Rev.* **D82** (2010) 034512, [`1004.4285`].

[129] K. Maltman, D. Leinweber, P. Moran and A. Sternbeck, *The realistic lattice determination of $\alpha_s(M_Z)$ revisited*, Phys. Rev. **D78** (2008) 114504, [`0807.2020`].

[130] [QCDSF/UKQCD 05] M. Göckeler, R. Horsley, A. Irving, D. Pleiter, P. Rakow, G. Schierholz et al., *A determination of the Lambda parameter from full lattice QCD*, *Phys.Rev.* **D73** (2006) 014513, [`hep-ph/0502212`].

[131] [SESAM 99] A. Spitz et al., *α_s from upsilon spectroscopy with dynamical Wilson fermions*, *Phys.Rev.* **D60** (1999) 074502, [`hep-lat/9906009`].

[132] M. Wingate, T. A. DeGrand, S. Collins and U. M. Heller, *From spectroscopy to the strong coupling constant with heavy Wilson quarks*, *Phys.Rev.* **D52** (1995) 307–319, [`hep-lat/9501034`].

[133] C. T. H. Davies, K. Hornbostel, G. Lepage, A. Lidsey, J. Shigemitsu et al., *A precise determination of α_s from lattice QCD*, *Phys.Lett.* **B345** (1995) 42–48, [`hep-ph/9408328`].

[134] S. Aoki, M. Fukugita, S. Hashimoto, N. Ishizuka, H. Mino et al., *Manifestation of sea quark effects in the strong coupling constant in lattice QCD*, *Phys.Rev.Lett.* **74** (1995) 22–25, [`hep-lat/9407015`].

[135] A. X. El-Khadra, G. Hockney, A. S. Kronfeld and P. B. Mackenzie, *A determination of the strong coupling constant from the charmonium spectrum*, *Phys.Rev.Lett.* **69** (1992) 729–732.

[136] [QCDSF/UKQCD 04A] M. Göckeler, R. Horsley, A. Irving, D. Pleiter, P. Rakow, G. Schierholz et al., *Determination of Λ in quenched and full QCD: an update*, *Nucl.Phys.Proc.Suppl.* **140** (2005) 228–230, [`hep-lat/0409166`].

[137] S. Booth, M. Göckeler, R. Horsley, A. Irving, B. Joo, S. Pickles et al., *The strong coupling constant from lattice QCD with $N_f = 2$ dynamical quarks*, *Nucl.Phys.Proc.Suppl.* **106** (2002) 308–310, [`hep-lat/0111006`].

[138] [QCDSF/UKQCD 01] S. Booth, M. Göckeler, R. Horsley, A. Irving, B. Joo, S. Pickles et al., *Determination of $\Lambda_{\overline{MS}}$ from quenched and $N_f = 2$ dynamical QCD*, *Phys.Lett.* **B519** (2001) 229–237, [`hep-lat/0103023`].

[139] [HPQCD 03A] C. T. H. Davies et al., *High-precision lattice QCD confronts experiment*, *Phys. Rev. Lett.* **92** (2004) 022001, [`hep-lat/0304004`].

[140] Q. J. Mason, *High-precision lattice QCD: Perturbations in a non-perturbative world*. PhD thesis, Cornell U., LNS, 2004.

[141] [HPQCD 08B] I. Allison et al., *High-precision charm-quark mass from current-current correlators in lattice and continuum QCD*, *Phys. Rev.* **D78** (2008) 054513, [`0805.2999`].

[142] A. Bochkarev and P. de Forcrand, *Determination of the renormalized heavy quark mass in lattice QCD*, *Nucl.Phys.* **B477** (1996) 489–520, [`hep-lat/9505025`].

[143] K. Chetyrkin, J. H. Kuhn and C. Sturm, *Four-loop moments of the heavy quark vacuum polarization function in perturbative QCD*, *Eur.Phys.J.* **C48** (2006) 107–110, [`hep-ph/0604234`].

[144] R. Boughezal, M. Czakon and T. Schutzmeier, *Charm and bottom quark masses from perturbative QCD*, *Phys.Rev.* **D74** (2006) 074006, [`hep-ph/0605023`].

[145] A. Maier, P. Maierhofer and P. Marqaurd, *The second physical moment of the heavy quark vector correlator at $O(\alpha_s^3)$*, *Phys.Lett.* **B669** (2008) 88–91, [`0806.3405`].

[146] A. Maier, P. Maierhofer, P. Marquard and A. Smirnov, *Low energy moments of heavy quark current correlators at four loops*, *Nucl.Phys.* **B824** (2010) 1–18, [`0907.2117`].

[147] Y. Kiyo, A. Maier, P. Maierhofer and P. Marquard, *Reconstruction of heavy quark current correlators at $O(\alpha_s^3)$*, *Nucl.Phys.* **B823** (2009) 269–287, [`0907.2120`].

[148] J. H. Kühn, M. Steinhauser and C. Sturm, *Heavy quark masses from sum rules in four-loop approximation*, *Nucl. Phys.* **B778** (2007) 192–215, [`hep-ph/0702103`].

[149] K. Chetyrkin, J. Kuhn, A. Maier, P. Maierhofer, P. Marquard et al., *Charm and Bottom Quark Masses: An Update*, *Phys.Rev.* **D80** (2009) 074010, [`0907.2110`].

[150] [HPQCD 13A] R. Dowdall, C. Davies, G. Lepage and C. McNeile, *V_{us} from π and K decay constants in full lattice QCD with physical u, d, s and c quarks*, *Phys.Rev.* **D88** (2013) 074504, [`1303.1670`].

[151] [HPQCD 10B] H. Na, C. T. H. Davies, E. Follana, G. P. Lepage and J. Shigemitsu, *The $D \to K\ell\nu$ semileptonic decay scalar form factor and $|V_{cs}|$ from lattice QCD*, *Phys.Rev.* **D82** (2010) 114506, [`1008.4562`].

[152] [HPQCD 12F] R.J. Dowdall, C. Davies, T. Hammant and R. Horgan, *Precise heavy-light meson masses and hyperfine splittings from lattice QCD including charm quarks in the sea*, *Phys. Rev.* **D86** (2012) 094510, [`1207.5149`].

[153] B. Dehnadi, A. H. Hoang and V. Mateu, *Bottom and Charm Mass Determinations with a Convergence Test*, *JHEP* **08** (2015) 155, [`1504.07638`].

[154] A. Cucchieri, *Gribov copies in the minimal Landau gauge: The Influence on gluon and ghost propagators*, *Nucl.Phys.* **B508** (1997) 353–370, [`hep-lat/9705005`].

[155] L. Giusti, M. Paciello, C. Parrinello, S. Petrarca and B. Taglienti, *Problems on lattice gauge fixing*, *Int.J.Mod.Phys.* **A16** (2001) 3487–3534, [`hep-lat/0104012`].

[156] A. Maas, J. M. Pawlowski, D. Spielmann, A. Sternbeck and L. von Smekal, *Strong-coupling study of the Gribov ambiguity in lattice Landau gauge*, *Eur.Phys.J.* **C68** (2010) 183–195, [`0912.4203`].

[157] B. Alles, D. Henty, H. Panagopoulos, C. Parrinello, C. Pittori et al., *α_s from the nonperturbatively renormalised lattice three gluon vertex*, *Nucl.Phys.* **B502** (1997) 325–342, [`hep-lat/9605033`].

[158] P. Boucaud, J. Leroy, H. Moutarde, J. Micheli, O. Pene et al., *Preliminary calculation of α_s from Green functions with dynamical quarks*, JHEP **0201** (2002) 046, [hep-ph/0107278].

[159] P. Boucaud, J. Leroy, A. Le Yaouanc, A. Lokhov, J. Micheli et al., *Asymptotic behavior of the ghost propagator in SU(3) lattice gauge theory*, *Phys.Rev.* **D72** (2005) 114503, [hep-lat/0506031].

[160] P. Boucaud, J. Leroy, A. Le Yaouanc, A. Lokhov, J. Micheli et al., *Non-perturbative power corrections to ghost and gluon propagators*, *JHEP* **0601** (2006) 037, [hep-lat/0507005].

[161] A. Sternbeck, K. Maltman, L. von Smekal, A. Williams, E. Ilgenfritz et al., *Running α_s from Landau-gauge gluon and ghost correlations*, *PoS* **LAT2007** (2007) 256, [0710.2965].

[162] Ph. Boucaud, F. De Soto, J. Leroy, A. Le Yaouanc, J. Micheli et al., *Ghost-gluon running coupling, power corrections and the determination of $\Lambda_{\overline{\text{MS}}}$*, *Phys.Rev.* **D79** (2009) 014508, [0811.2059].

[163] [ETM 13D] B. Blossier et al., *High statistics determination of the strong coupling constant in Taylor scheme and its OPE Wilson coefficient from lattice QCD with a dynamical charm*, *Phys.Rev.* **D89** (2014) 014507, [1310.3763].

[164] [ETM 12C] B. Blossier, P. Boucaud, M. Brinet, F. De Soto, X. Du et al., *The strong running coupling at τ and Z_0 mass scales from lattice QCD*, *Phys.Rev.Lett.* **108** (2012) 262002, [1201.5770].

[165] [ETM 11D] B. Blossier, P. Boucaud, M. Brinet, F. De Soto, X. Du et al., *Ghost-gluon coupling, power corrections and $\Lambda_{\overline{\text{MS}}}$ from lattice QCD with a dynamical charm*, *Phys.Rev.* **D85** (2012) 034503, [1110.5829].

[166] A. Sternbeck, K. Maltman, M. Müller-Preussker and L. von Smekal, *Determination of $\Lambda_{\overline{\text{MS}}}$ from the gluon and ghost propagators in Landau gauge*, *PoS* **LAT2012** (2012) 243, [1212.2039].

[167] A. Sternbeck, E.-M. Ilgenfritz, K. Maltman, M. Müller-Preussker, L. von Smekal et al., *QCD Lambda parameter from Landau-gauge gluon and ghost correlations*, *PoS* **LAT2009** (2009) 210, [1003.1585].

[168] [ETM 10F] B. Blossier et al., *Ghost-gluon coupling, power corrections and $\Lambda_{\overline{\text{MS}}}$ from twisted-mass lattice QCD at $N_f = 2$*, *Phys.Rev.* **D82** (2010) 034510, [1005.5290].

[169] E.-M. Ilgenfritz, C. Menz, M. Müller-Preussker, A. Schiller and A. Sternbeck, *SU(3) Landau gauge gluon and ghost propagators using the logarithmic lattice gluon field definition*, *Phys.Rev.* **D83** (2011) 054506, [1010.5120].

[170] F. De Soto and J. Rodriguez-Quintero, *Notes on the determination of the Landau gauge OPE for the asymmetric three gluon vertex*, *Phys.Rev.* **D64** (2001) 114003, [hep-ph/0105063].

[171] P. Boucaud, A. Le Yaouanc, J. Leroy, J. Micheli, O. Pene et al., *Testing Landau gauge OPE on the lattice with a $\langle A^2 \rangle$ condensate*, *Phys.Rev.* **D63** (2001) 114003, [hep-ph/0101302].

[172] P. Boucaud, A. Le Yaouanc, J. Leroy, J. Micheli, O. Pene et al., *Consistent OPE description of gluon two point and three point Green function?*, *Phys.Lett.* **B493** (2000) 315–324, [hep-ph/0008043].

[173] P. Boucaud, G. Burgio, F. Di Renzo, J. Leroy, J. Micheli et al., *Lattice calculation of $1/p^2$ corrections to α_s and of $\Lambda_{\rm QCD}$ in the MOM scheme*, *JHEP* **0004** (2000) 006, [hep-ph/0003020].

[174] D. Bećirević, P. Boucaud, J. Leroy, J. Micheli, O. Pene et al., *Asymptotic scaling of the gluon propagator on the lattice*, *Phys.Rev.* **D61** (2000) 114508, [hep-ph/9910204].

[175] D. Bećirević, P. Boucaud, J. Leroy, J. Micheli, O. Pene et al., *Asymptotic behavior of the gluon propagator from lattice QCD*, *Phys.Rev.* **D60** (1999) 094509, [hep-ph/9903364].

[176] P. Boucaud, J. Leroy, J. Micheli, O. Pene and C. Roiesnel, *Three loop beta function and nonperturbative α_s in asymmetric momentum scheme*, *JHEP* **9812** (1998) 004, [hep-ph/9810437].

[177] P. Boucaud, J. Leroy, J. Micheli, O. Pene and C. Roiesnel, *Lattice calculation of α_s in momentum scheme*, *JHEP* **9810** (1998) 017, [hep-ph/9810322].

[178] [ETM 13] K. Cichy, E. Garcia-Ramos and K. Jansen, *Chiral condensate from the twisted mass Dirac operator spectrum*, *JHEP* **1310** (2013) 175, [1303.1954].

[179] K. G. Chetyrkin and J. H. Kuhn, *Quartic mass corrections to R(had)*, *Nucl. Phys.* **B432** (1994) 337–350, [hep-ph/9406299].

[180] J.-L. Kneur and A. Neveu, *Chiral condensate from renormalization group optimized perturbation*, *Phys. Rev.* **D92** (2015) 074027, [1506.07506].

[181] [CERN 08] L. Giusti and M. Lüscher, *Chiral symmetry breaking and the Banks–Casher relation in lattice QCD with Wilson quarks*, *JHEP* **03** (2009) 013, [0812.3638].

[182] [JLQCD 16B] G. Cossu, H. Fukaya, S. Hashimoto, T. Kaneko and J.-I. Noaki, *Stochastic calculation of the Dirac spectrum on the lattice and a determination of chiral condensate in 2+1-flavor QCD*, *PTEP* **2016** (2016) 093B06, [1607.01099].

[183] [ALPHA 14A] M. Bruno, J. Finkenrath, F. Knechtli, B. Leder and R. Sommer, *Effects of Heavy Sea Quarks at Low Energies*, *Phys. Rev. Lett.* **114** (2015) 102001, [1410.8374].

[184] A. Athenodorou, J. Finkenrath, F. Knechtli, T. Korzec, B. Leder, M. K. Marinkovic et al., *How perturbative are heavy sea quarks?*, *Nucl. Phys.* **B943** (2019) 114612, [1809.03383].

[185] Particle Data Group collaboration, C. Patrignani et al., *Review of Particle Physics*, *Chin. Phys.* **C40** (2016) 100001.

[186] Particle Data Group collaboration, J. Beringer et al., *Review of Particle Physics*, *Phys.Rev.* **D86** (2012) 010001 and 2013 partial update for the 2014 edition.